K2K Experiment – Internal Note: Dermination of the axial vector mass M_A with the Scintillating Fiber detector

Richard Gran

University of Washington

Eun Ju Jeon

Institute of Particle and Nuclear Studies,

*High Energy Accelerator Research Organization(KEK)**

For the SciFi detector group

(Dated: November 8, 2004)

Abstract

We have studied the neutrino-oxygen quasi-elastic scattering, $\nu_\mu + n \to \mu^- + p$, in the few GeV region using events from the Scintillating Fiber detector in the K2K neutrino beam. We determined the axial-vector mass, M_A, under the assumption of a dipole parametrization of the axial vector form factor and conserved vector current hypothesis. We present data for two data sets: $M_A = 1.21 \pm 0.15$ syst. $\pm$ 0.03 stat. for K2K-I data and $M_A = 1.20 \pm 0.18$ syst. $\pm$ 0.04 stat. for K2K-IIa data. This is the first estimation of the axial-vector mass in oxygen and the value is consistent with previous measurements with different targets. We have quantitatively considered systematic errors due to the quasi-elastic form factors and nuclear effects such as the Pauli blocking, nuclear rescattering, and the nucleon momentum distribution.

PACS numbers: 13.15.+g; 23.40.Bw; 25.30.Pt

*Now at Seoul National University(ejjeon@phya.snu.ac.kr)

I. INTRODUCTION

The structure of the nucleon, as measured both by electrons and neutrinos, has been a subject of experimental study for many years. The discovery of neutrino oscillations has renewed interest in neutrino interactions. There are currently many new experimental programs studying this topic, as well as progress on the theoretical calculations. The study described here focuses on the quasi-elastic cross-section and the shape of the q^2 (square of the lepton momentum transfer) distribution in neutrino-Oxygen interactions. This is the first estimation of this for Oxygen nuclei. In this paper we also present a quantitative study of the effects of the nucleus, such as the Pauli exclusion principle, the nucleon momentum distribution, and the effects of nuclear rescattering of recoil protons.

The neutrino quasi-elastic cross section, $d\sigma/dq^2(\nu_\mu + n \rightarrow \mu^- + p)$, is parameterized as described in Smith [3] in terms of the vector and the axial-vector form factors. The vector form factors have been measured in electron scattering experiments and can be parameterized with a dipole form factor $(1 + q^2/M_V^2)^{-2}$, where q^2 is the lepton momentum transfer squared, with a vector mass M_V=0.84 GeV/c^2. Recent measurements at SLAC and JLAB show that the vector form factors differ from the dipole form and new, more accurate parameterizations have been suggested [12–14]; this new information is considered in this analysis.

Since the vector form factors are accurately determined by the electron scattering experiments, the neutrino quasi-elastic scattering is described by only two other experimentally measured distributions: the axial-vector and pseudo-scalar form factors. The axial vector form factor is typically parameterized using a dipole form with a single parameter, the axial-vector mass M_A. The pseudo-scalar form factor contributes negligibly for electron and muon neutrino interactions at these energies.

In order to obtain the neutrino spectrum for the oscillation analysis [10] or other high precision neutrino experiments, we need to know the neutrino-oxygen quasi-elastic and inelastic cross sections. These cross-sections are modified from their free-nucleon form to account for the effects of the nucleus, as Smith and Moniz [2] and Rein and Sehgal[4] do with a Fermi-gas model. Because most current and proposed experiments use nuclear targets, these modifications are an active area of study, and have been the subject of three recent workshops on neutrino-nucleus interactions, NuInt01, NuInt02, and NuInt04. We will estimate the axial

vector mass for quasi-elastic interactions in this note. We also quantitatively estimate the type and magnitude of the expected nuclear effects and how they affect this measurement.

II. QUASI-ELASTIC SCATTERING CROSS SECTION AND FORM FACTORS

The differential cross section is written as

$$\frac{d\sigma^{\nu(\bar{\nu})}}{dq^2} = \frac{M^2 G_F^2 \cos^2\theta_c}{8\pi E_\nu^2}\left[A(q^2) \mp B(q^2)\frac{s-u}{M^2} + C(q^2)\frac{(s-u)^2}{M^4}\right] \tag{1}$$

where, s and u are Mandelstam variables: (s-u) = 4ME_ν - q^2 - m^2, m is the outgoing lepton mass and E_ν is the neutrino energy.[3]
$A(q^2)$, $B(q^2)$, and $C(q^2)$ are written as,

$$\begin{aligned}
A(q^2) &= \frac{m^2-q^2}{4M^2}[(4-\frac{q^2}{M^2})|F_A|^2 - (4+\frac{q^2}{M^2})|F_V^1|^2 - \frac{q^2}{M^2}|\xi F_V^2|^2(1+\frac{q^2}{4M^2}) \\
&\quad -\frac{4q^2 F_V^1 \xi F_V^2}{M^2} - \frac{m^2}{M^2}((F_V^1+\xi F_V^2)^2 + |F_A|^2)] \\
B(q^2) &= \frac{q^2}{M^2}(F_A(F_V^1+\xi F_V^2)) \\
C(q^2) &= \frac{1}{4}(|F_A|^2 + |F_V^1|^2 - \frac{q^2}{4M^2}|\xi F_V^2|^2)
\end{aligned} \tag{2}$$

$F_V^1(q^2)$ and $F_V^2(q^2)$ are the Dirac electromagnetic isovector form factor and the Pauli electromagnetic isovector form factor, respectively and vector mass M_V is set to be 0.84 GeV/c^2. These formulae assume the conserved vector current (CVC) hypothesis, which allows us to write F^1 and F^2 in terms of the well measured Sachs form factors G_E^P, G_E^N, G_M^P, and G_M^N.

In analogy with the electromagnetic form factors, the axial vector form factor, F_A, is presumed to obey the "dipole" formula, at least approximately:

$$F_A(q^2) = -\frac{1.26}{(1-(q^2/M_A^2))^2}. \tag{3}$$

Previous studies [18] show that this parameterization is reasonable.

With F_V accurately measured, the differential cross section is reduced to formula which is a function of the neutrino energy E_ν, the four-momentum transfer q^2, with one unknown parameter, M_A. This parameter can be determined by studying the q^2 distribution observed in the data from the SciFi detector.

A. Nuclear Effects

Equation 1 is the differential cross section for the *free* neutron, and must be modified to account for the effects of a neutron bound in a nucleus. In the SciFi detector, the target neutrons are in Oxygen and Aluminum, though other detectors in K2K and other experiments are concerned about a variety of targets, including Iron, Lead, Argon, and Carbon.

The primary deviation from the free neutron cross section is due to the Pauli exclusion principle and the momentum distribution of nucleons in the target nucleus. After a quasi-elastic interaction the momentum of the recoil proton could be the same as another proton in the nucleus (same quantum state), and that interaction can not proceed due to the Pauli exclusion principle. Pauli-blocking also affects delta-resonance production in a similar way. The result is a suppression of interactions with momentum transfer $q^2 < 0.2$ GeV^2, shown in Fig. 1 for a calculation of the quasi-elastic cross-section.

The nucleus has a variety of other, smaller effects on the cross-section and kinematics of these interactions. There is now much theoretical work on these topics and several experiments will explore neutrino interactions on nuclei with more precision in the next decade. In the section on systematic effects, we summarize some of the calculations and discuss the magnitude of their effect on the shape of the q^2 distributions used in the MA analysis.

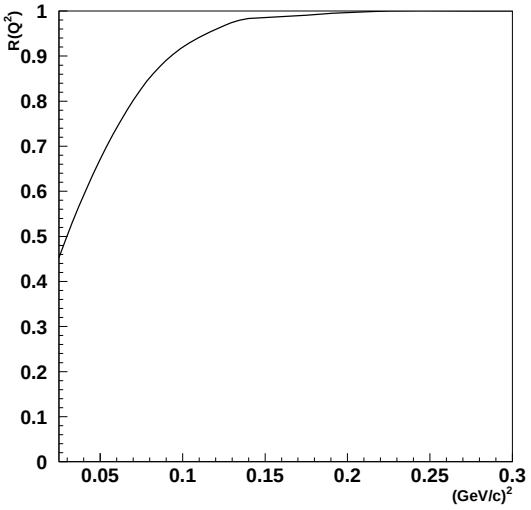

FIG. 1: Correction factor for the differential cross section to account for the Pauli exclusion priciple and Fermi motion in the oxygen nucleus.

III. DATA SAMPLE

As of this writing, the data sample includes the K2K-I data (November 1999 to July 2001) which had the lead glass detector between SciFi and MRD, and the K2K-IIa data (January to June 2003) which had the four-layer prototype for the SciBar detector in place of the lead glass. A third set of data, K2K-IIb (October 2003 to February 2004) was taken with the full SciBar detector; the SciFi data is currently being analyzed. A fourth running period, K2K-IIc began in October 2004 with a SciFi detector emptied of its water and with aluminum rods filling many of the tanks. The SciFi detector is described in more detail in [19].

We have chosen events whose vertex begins in the SciFi detector fiducial volume and have at least one track penetrate to the Muon Range Detector (MRD). With this requirement, the long track is usually a muon and thus we select primarily charged current interactions. The K2K-IIa data includes only events that penetrate two X and two Y layers into the MRD. For the K2K-I data, the lead glass provides enough extra material that we include interactions with a track that just hits the first layer of the MRD (MRD-1L events) and still maintain high muon purity while accepting lower energy events. Some significant fraction of events leave one hit, but not two hits in the second XY layer of the MRD, while an additional 15% of events have a track that penetrates significantly (two to five layers) into the MRD, but only had a reconstructed track in the X or Y projection, but not both. This last category is not included in the analysis at this time.

Under these conditions, the muon momentum threshold for detecting the muon for K2K-I data is around 675 MeV, while for K2K-IIa it is slightly lower, about 550 MeV. Both these values are estimated as the momentum where the event rate is approximately half the peak rate. There is some acceptance for muons about 100 MeV lower than these values.

A. Calculating q^2 and E_ν and SciFi detector resolution

The kinematics of the muon (the longest track in the event) are sufficient to estimate the energy of the neutrino, E_ν and the square of the energy transfer q^2, assuming the event is quasi-elastic.

$$E_\nu = \frac{(m_N + B)E_\mu - (2m_N B + B^2 + m_\mu^2)/2}{m_N + B - E_\mu + p_\mu \cos\theta_\mu},$$

quantity	mean sigma units (true - reconstructed)
muon momentum	-0.0102 0.116 GeV/c
muon angle	0.0046 0.786 degrees
neutrino energy	-0.0042 0.161 GeV
q^2	0.0011 0.052 $(GeV/c)^2$

TABLE I: Resolution (sigma) and also the mean of the true - reconstructed distribution for different quantities with the SciFi detector. These are approximate, and based on a Gaussian fit.

$$-q^2 = -2E_\nu(E_\mu - p_\mu \cos\theta_\mu) + m_\mu^2.$$

Here, E_μ and p_μ are the energy and momentum of the muon, determined from the range, θ_μ is the angle determined from the hits in the SciFi detector. Also B is the nucleon binding energy, -30 MeV for oxygen, m_N and m_μ are the neutron and muon mass, E_μ and θ_μ are measured with 3% accuracy in the MRD detector and 2-3 degrees with the SciFi detector, respectively. Finally, this formula assumes that the target neutron inside the nucleus is at rest, ignoring the momentum distribution for this calculation.

The important quantities for this analysis are the muon momentum, muon angle, and the derived reconstructed neutrino energy and q^2 for each event. The event-by-event resolution for these quantities is given in Tab. I and the distributions are shown in Fig. 2. These data include all events in the one-track and two-track samples. The neutrino energy and q^2 resolution are calculated after selecting QE events from this sample. These distributions do not yet include a momentum shift that we apply at the analysis stage to account for the shifted mean.

For non-QE events, the calculation is systematically wrong because of the QE assumption. The actual resolution for these events is checked by assuming the production and decay of a delta resonance and proceeding with a slightly different calculation:

$$E_\nu = \frac{m_N E_\mu + (\Delta^2 - m_N^2 - m_\mu^2)/2}{m_N - E_\mu + p_\mu \cos\theta_\mu},$$

In this case, the resolution is similar [include actual numbers here soon], though it will still not be correct for multi-pion or deep inelastic scattering. However, we can not identify QE from non-QE on an event by event basis, but for analyses that fit data to MC the resulting

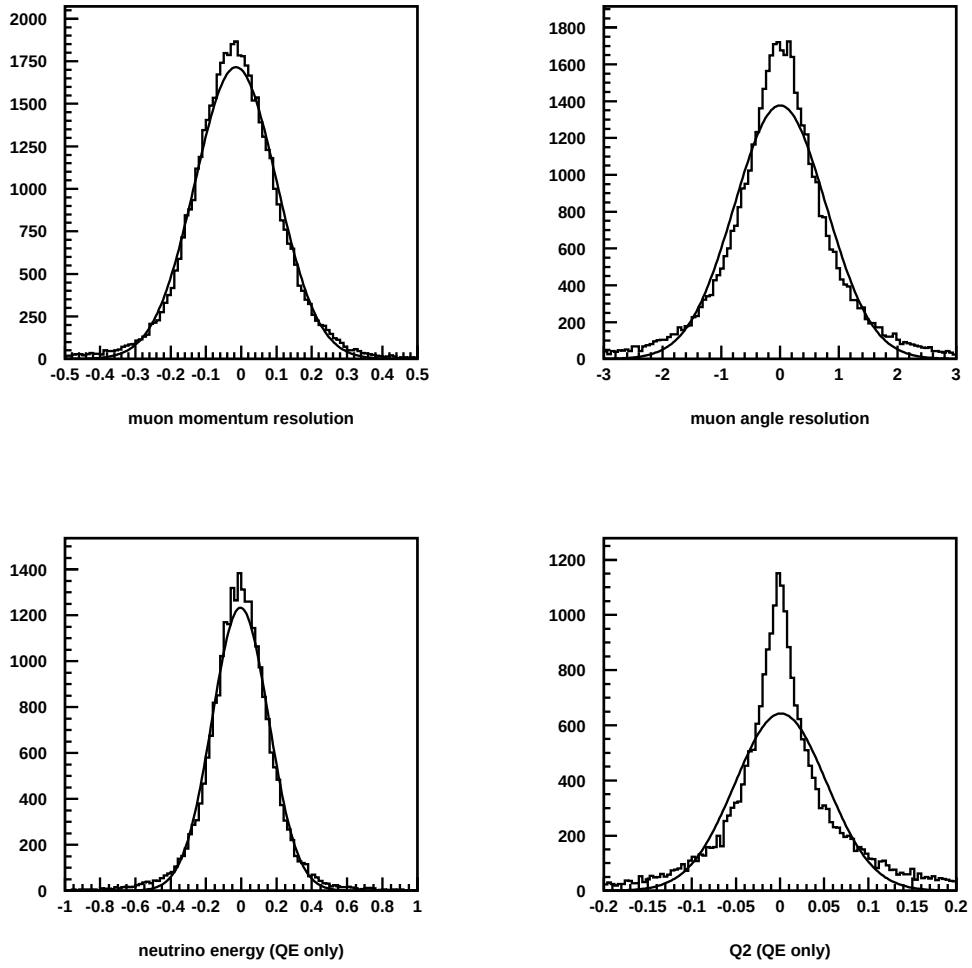

FIG. 2: SciFi detector resolution for p_μ, θ_μ, E_ν, and q^2. Each distribution is true - reconstructed, from MC The mean and sigma from the Gaussian fit are given in Tab. I.

error is negligible because the data and MC are treated the same way. One important observation, the error introduced by the QE assumption causes non-QE events to be reconstructed at low q^2.

B. Data subsamples

The value for M_A is determined from the q^2 distributions of three sub-samples of SciFi detector data: 1-track, 2-track quasi-elastic enhanced (QE), and 2-track non-quasi-elastic enhanced (nonQE) samples. In order to be accepted as a second track, we require the

particle to produce hits in at least three layers in the SciFi detector. This requirement is equivalent to a momentum threshold of about 600 MeV/c for protons.

The two track sample is divided in the following way. For quasi-elastic events, the direction of the recoil proton can be predicted from the kinematics of the observed muon. Events whose observed second track is within 25 degrees of this prediction are likely to be quasi-elastic. The second track for non-quasi-elastic events should be distributed among a wider range of angles relative to this prediction, so the sample whose second track is greater than 25 degrees has enhanced non-quasi-elastic events. The effectiveness of this cut is demonstrated in figure [add figure], and the purity of these samples in Table. II.

Percent purity	K2K-I	K2K-IIa
1-track	60	57
2-track QE	61	58
2-track nonQE	15	12

TABLE II: Quasi-elastic purity (percent) of the data sub-samples in this analysis.

In Tab. III the number of events from three categories is shown with no minimum q^2 cut and with the standard $q^2 > 0.2(GeV/c)^2$ cut.

	K2K-I		K2K-IIa	
q^2 $(GeV/c)^2$	$q^2 > 0.0$	$q^2 > 0.2$	$q^2 > 0.0$	$q^2 > 0.2$
1 track	5958	2849	3617	1500
2 track QE	764	674	451	372
2 track nonQE	1286	659	904	437

TABLE III: Number of events in three event samples used for M_A measurement.

The purity of the one-track and the two-track QE enhanced samples is about 60% QE, while the two-track nonQE sample has only 15% QE events in it. Using these three event samples in a combined fit, the fit procedure can identify the ratio of QE signal and non-QE background for all three samples.

C. Small angle deficit

We observe a significant deficit of events at angles near the direction of the beam in data from all K2K near detectors. There are several pieces of the neutrino interaction model and nuclear effects that have known large uncertainties which could be the source of this discrepancy. The application of Pauli Blocking in the Fermi Gas model, especially for resonant pion events, and also the cross-section for coherent pion production are two examples. Other aspects of the nuclear interaction model are uncertain and the actual cause may be something different entirely.

The discrepancy is illustrated with the SciFi data sets shown in Fig. 3. K2K-I data includes MRD-3D and 1L events, while K2K-IIa data includes only MRD-3D events. These data are the unweighted data sets, they do not include the Bodek/Yang DIS re-weighting, the Marteau coherent pion correction, or the spectrum-fit re-weighting. The first two will lessen the apparent discrepancy. I will regenerate the plots with these re-weighting factors shortly.

Our detectors directly measure the lepton angle, but most aspects of the cross-section calculation for these interaction modes are naturally expressed as a function of q^2. This is true of the cross-section itself, as well as Pauli blocking. As seen in the equations in the previous section, the calculation of E_ν and q^2 involve only functions of p_μ and $\cos\theta_\mu$. The M_A fits in this analysis will use only data with $\mathrm{q}^2 > 0.2$, effectively avoiding the apparent discrepancy. One caution remains: because the cause of the discrepancy is not known, there could be a small effect at higher angles and higher q^2 which is not apparent from these distributions, but which might contribute a systematic error to the M_A analysis. Some of these causes are explored quantitatively in later sections.

IV. PROCEDURE FOR FITTING M_A

In Fig. 4 the theoretical predictions of the differential cross section for neutrinos on oxygen target, $d\sigma/dq^2$ for three values of M_A=1.0, 1.1, and 1.2 GeV/c^2 at the energy of E_ν=1.3 GeV are shown. As can be seen in the left plot of Figure 4, the absolute cross section is almost proportional to the M_A value. The figure on the right is normalized by area and shows that there are significant differences in the shapes with the same choices of M_A.

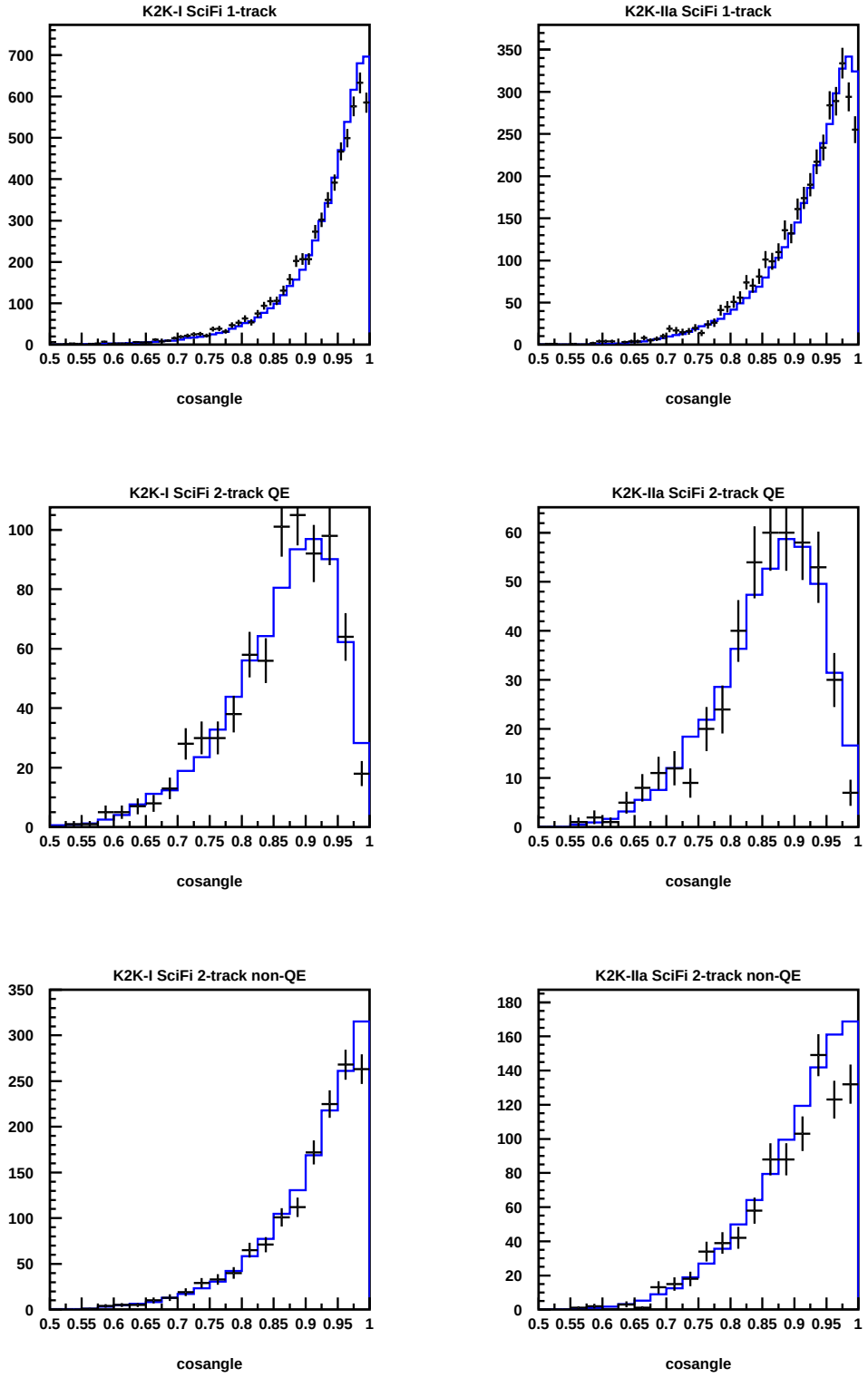

FIG. 3: Small angle discrepancy, shown as a deficit at values of $\cos\theta$ near 1. These are raw distributions, no Bodek/Yang, no Marteau, no Spectrum Fit.

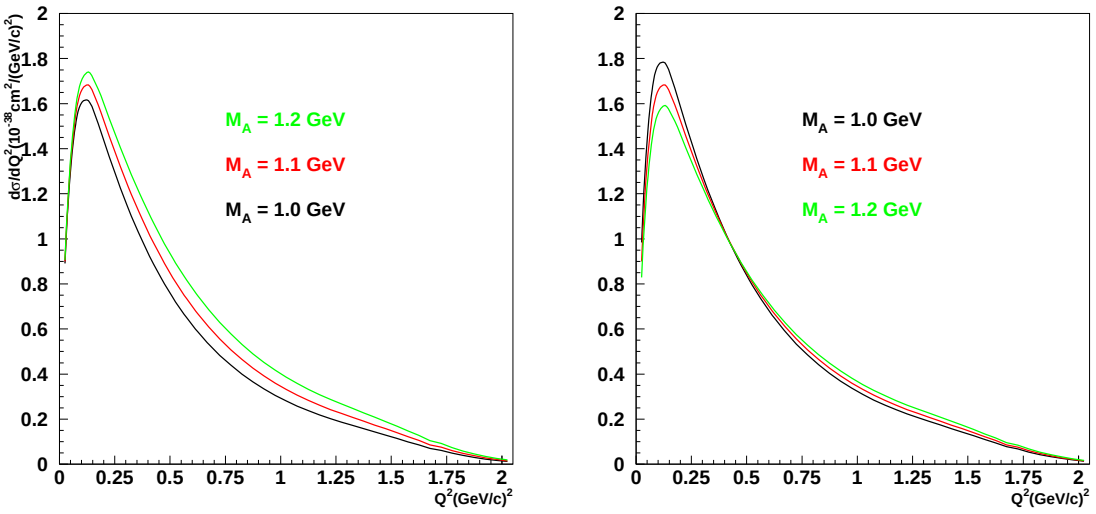

FIG. 4: Left: theoretical predictions of the differential cross section $d\sigma/dq^2$ for the values of M_A=1.0, 1.1, and 1.2 GeV/c^2. Right: the same three distributions, normalized by area.

A. Likelihood function

In the present analysis, we are consider only the shape of the q^2 distributions. In this case we are not sensitive to the overall uncertainty in the cross section, nor to uncertainties due to the absolute neutrino flux or the number of target nucleons in the SciFi fiducial volume. To determine the best value of M_A we have performed maximum-likelihood fit to data. In the likelihood fit we minimize:

$$NegativeLogLikelihood = -\log \prod \mathbf{P}(N_{ij}^{Observed}, N_{ij}^{Expected})$$

Where, $\mathbf{P}$ is the result from Poisson statistics, $N_{ij}^{Obs.}$ and $N_{ij}^{Expected}$ are the number of measured and expected events in the bins of (E_{ν_i}, q_j^2), respectively. We used the shape of q^2 distribution for each observed neutrino energy in 5 bins such as (0.5-1.0), (1.0-1.5), (1.5-2.0), (2.0-2.5), and (2.5-4.0) (GeV). The q^2 distribution uses bins with a width of $0.1(GeV/c)^2$. We use the approximation for Poisson statistics [20] which requires some minimum statistics per bin, and we have combined bins at high energy and high q^2 to meet this requirement.

Here, the number of expected events $N_{ij}^{Exp.}$ in the bins of (E_{ν_i}, q_j^2), is calculated by combining the theoretical cross-section for Quasi-elastic events, the inelastic events from the NEUT Monte Carlo, and the detector resolution and acceptance.

$$N^{expect}(E,q^2) = A\Big[flux(E)\times d\sigma/dq^2(E,M_A,q^2)\times R(E,q^2) + B\times InelasticBackgrd(E,q^2)\Big]$$

A is an overall normalization factor, B is the relative inelastic fraction with respect to the QE fraction, and R(E,q^2) is a correction factor due to nuclear effects. There are actually five free parameters included in flux(E) for the overall normalization for each of five energy ranges; within a particular energy range, the flux (equivalently, the shape of the energy spectrum) is taken from the official Monte Carlo. In this way we separately consider the shape of the q^2 distribution for each energy range. For the primary analysis flux(E) is not constrained. A secondary analysis, described in section V-E, constrains these by including the best fit parameter and errors from the Summer 2004 near detector merged fit results.

This equation simplifies one aspect of the calculation; it does not include the information about the detector acceptance and resolution. Instead of a simple factor for this, a complete migration is calculated from the Monte Carlo and expressed in the form of a migration matrix $M(E_{true}, q^2_{true} \rightarrow N_{track}, E_{rec}, q^2_{rec})$, where one variable refers to the one-track, two-track QE, or two-track non-QE sample. Each entry in this matrix specifies how many events migrate from that bin to the other neighboring bins and also the detector acceptance, all at once. This is applied to the calculated cross section as follows:

$$N_{QE}(N_{track}, E_{rec}, q^2_{rec}) = \sum_{(E_{true},q^2_{true})}^{allbins} flux{*}d\sigma/dq^2(E_{true}, q^2_{true})\times M(E_{true}, q^2_{true} \rightarrow N_{track}, E_{rec}, q^2_{rec})$$

The shape of the non-quasi-elastic background is taken directly from the Neut Monte Carlo and our detector acceptance, and there is only one free parameter to describe the relative normalization of quasi-elastic and inelastic. The values for flux(E) free parameters are also applied. The uncertainties in the shape of this background have a significant effect on the shape of the quasi-elastic signal and the fit value for MA; these uncertainties are considered separately and described in section VI. In particular, the cross-section for single pion production involves its own axial vector mass, $M_A^{1\pi}$, which is taken to be 1.1 in our Monte Carlo.

Because the most significant effect of the nucleus is Pauli blocking, and because this only applies to the low q^2 region, we do not include these data in the fit. Further, all the near detectors in the K2K experiment see a significant deficit of events at low q^2 and/or at very

forward angles, which is excluded with the same cut. Analysis of this deficit is currently under study.

V. RESULTS AND DISCUSSION

The results from the fit just described are shown here for the K2K-I and K2K-IIa data separately. In each plot on the following pages I have shown the data, the best fit MC, and the QE fraction reported by the best fit. The data are broken all the way down to the fifteen samples: one track, two-track QE, two-track non-QE $\times$ five energy regions. With each data sample is a summary of the results from the fit, including the fit value for flux(E) parameters ("SPECTRUM"), and the chisquare for the fit.

A. K2K-I results: 1.21 ± 0.15 syst. ± 0.03 stat.

The data distributions, with the best fit Monte Carlo are shown in the following plots.

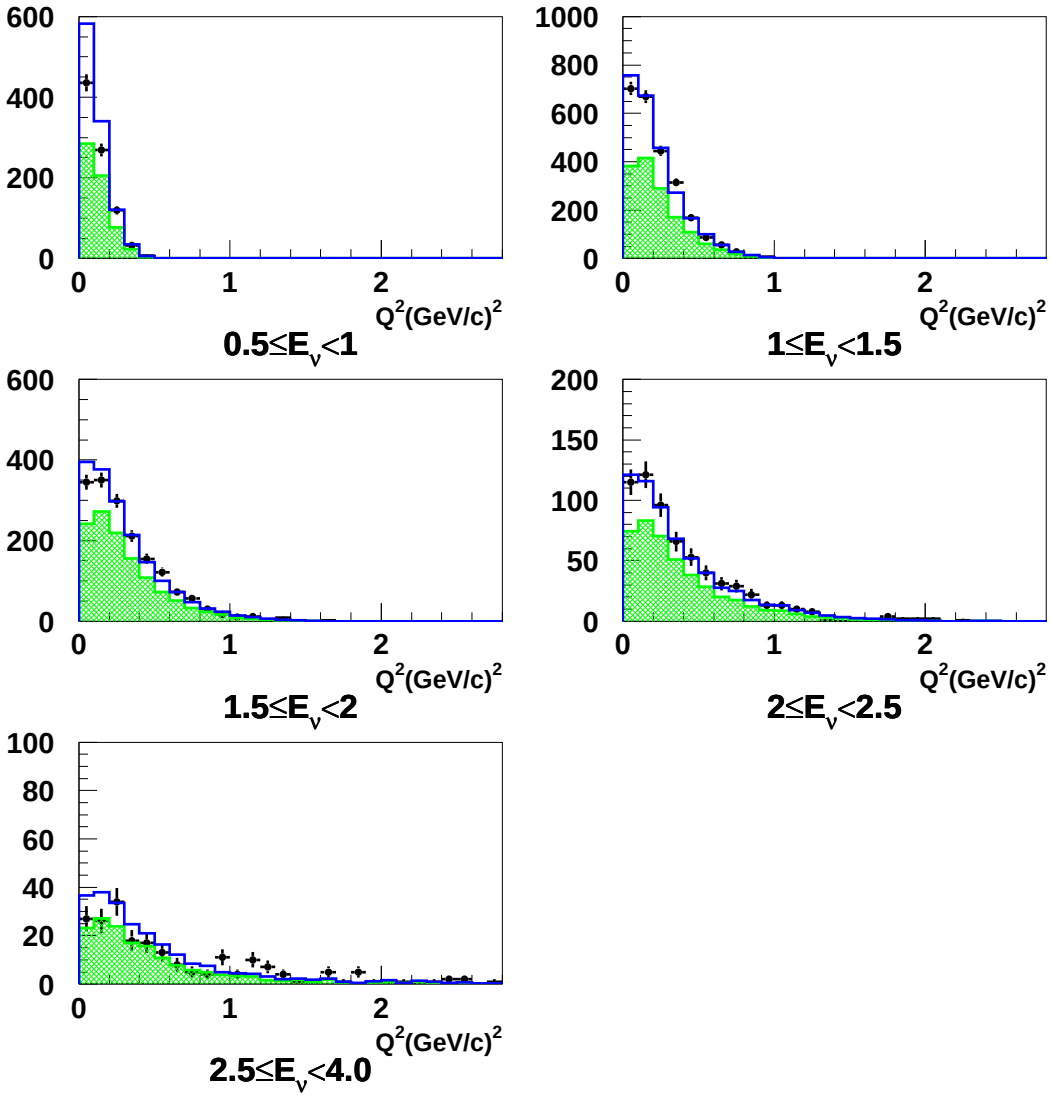

FIG. 5: K2K-I 1-track q^2 distributions for each observed neutrino energy with the best fit M_A

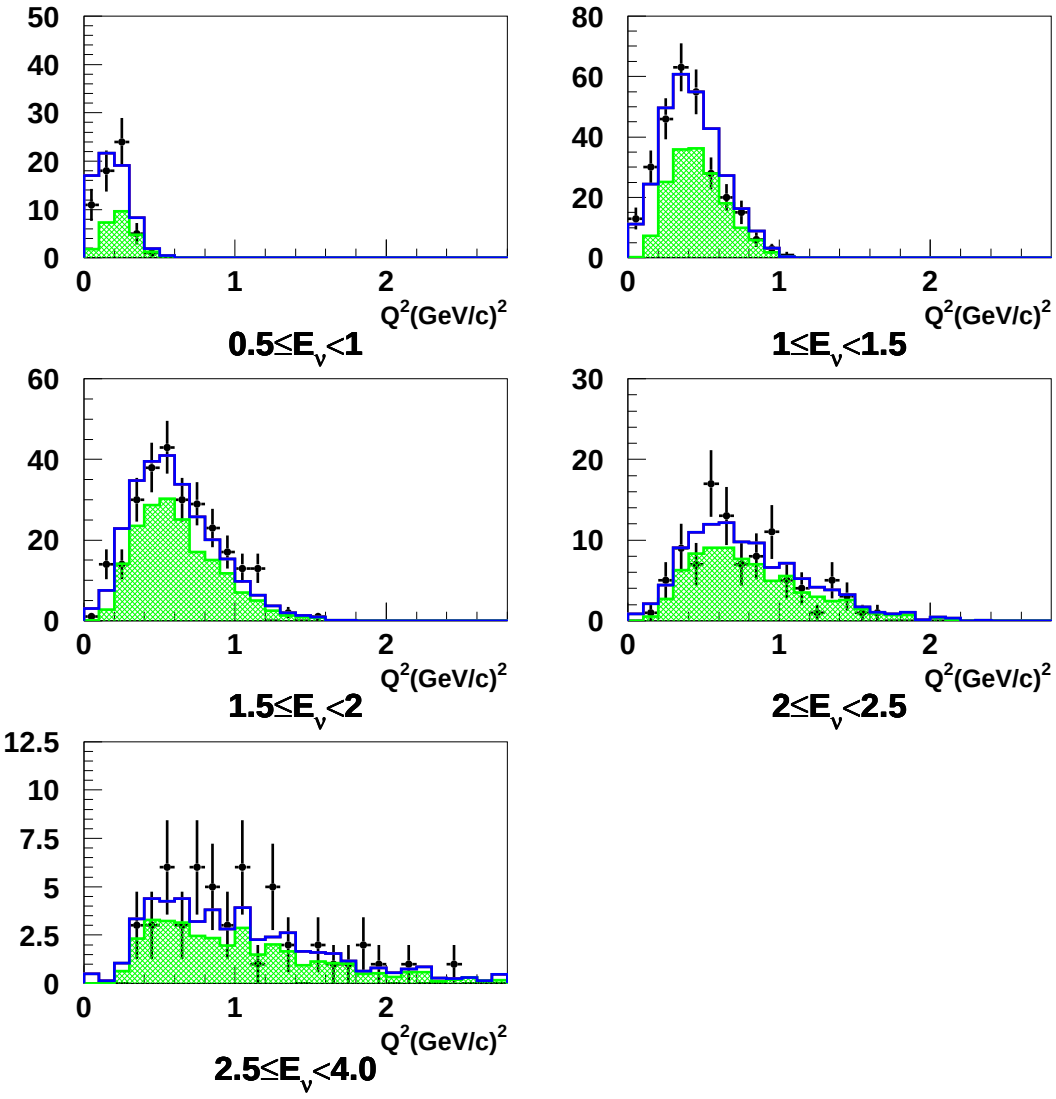

FIG. 6: K2K-I 2-track QE q^2 distributions for each observed neutrino energy with the best fit M_A

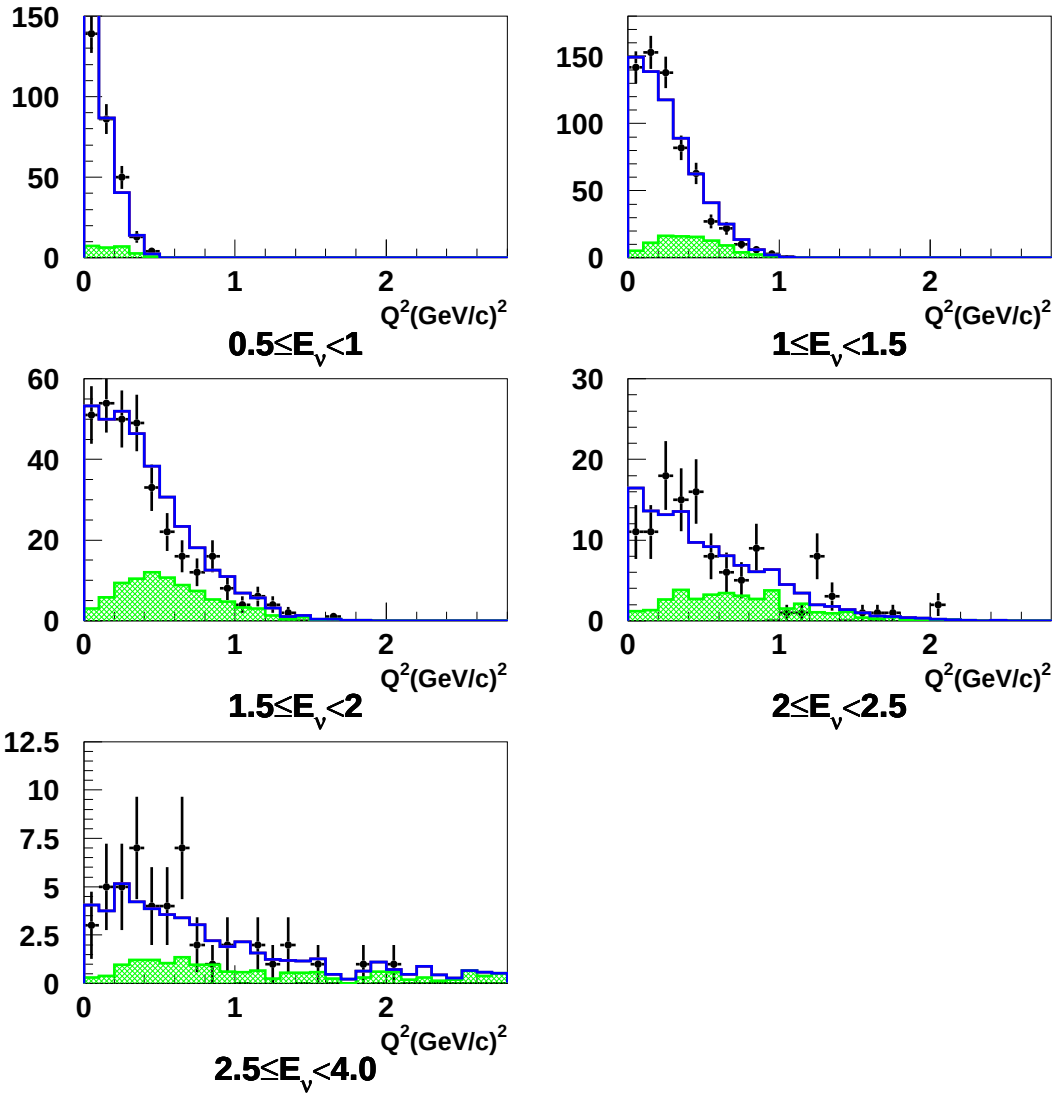

FIG. 7: K2K-I 2-track nonQE q^2 distributions for each observed neutrino energy with the best fit M_A

Table of parameters from the fit and also the input parameters.

```
 mrdescale=  0.950
 LGweight=   0.950
 Chisqr =   172.205338
 Chisqr/NDOF =   1.3776427 125
```

	Value	+Err	-Err	ErrPara	Corr
MA	1.214480	0.098887	-0.095875	0.106859	0.962954
SPECTRUM	2.140657	0.410045	-0.382515	0.404016	0.722409
SPECTRUM	0.875348	0.106113	-0.097323	0.104915	0.918014
SPECTRUM	1.025762	0.115484	-0.102604	0.116377	0.951915
SPECTRUM	0.873036	0.124149	-0.112216	0.122151	0.889302
SPECTRUM	1.222631	0.179167	-0.156272	0.177911	0.889454
PROTON_RES	1.040832	0.072125	-0.072445	0.072866	0.331452
QE/nQE	1.076252	0.132192	-0.118849	0.135670	0.960197

(note, the non-QE/QE is not exactly correct yet, but does not affect the fit)

B. K2K-IIa results: 1.20 ± 0.18 syst. ± 0.04 stat.

The data distributions, with the best fit Monte Carlo are shown in the following plots.

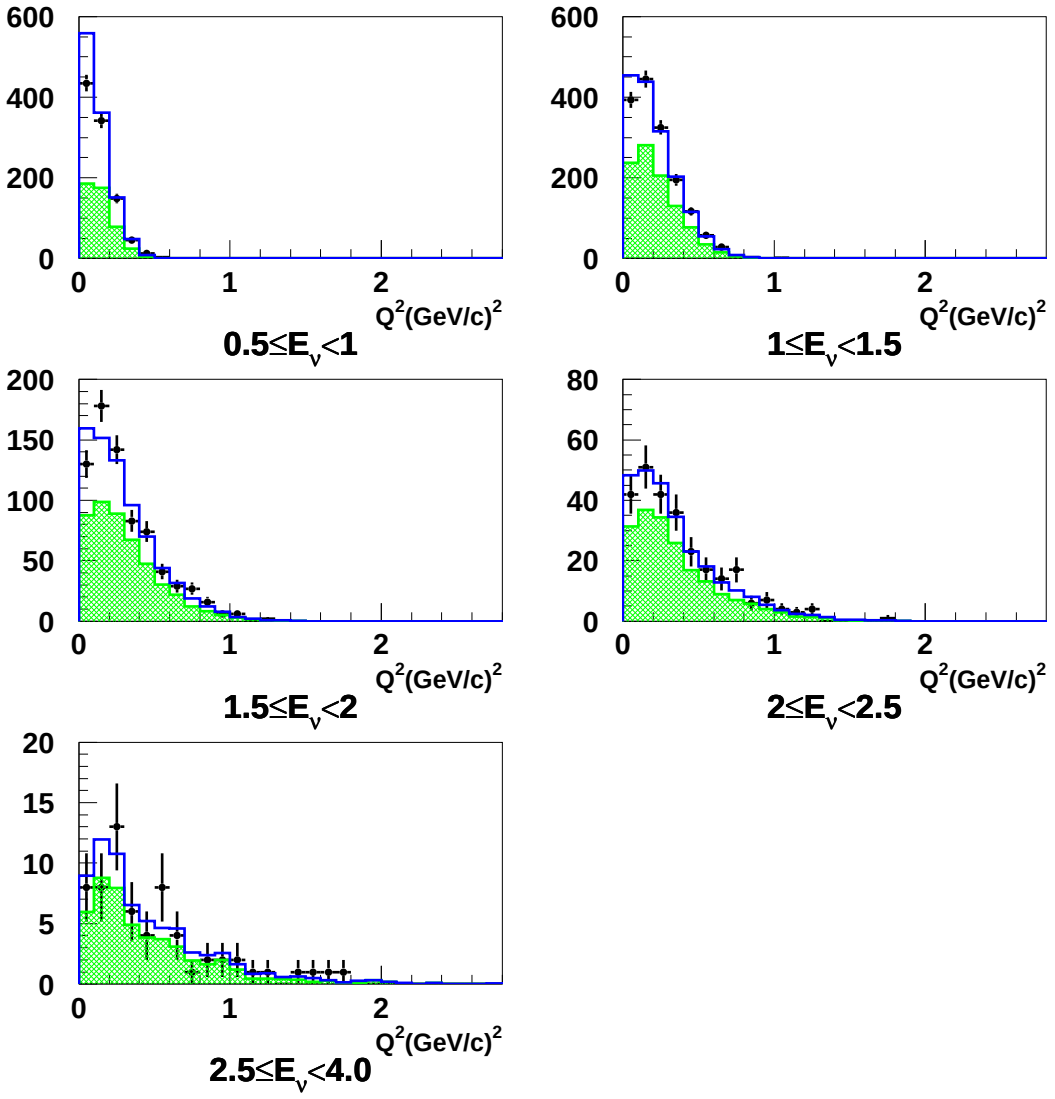

FIG. 8: K2K-IIa 1-track q^2 distributions for each observed neutrino energy with the best fit M_A

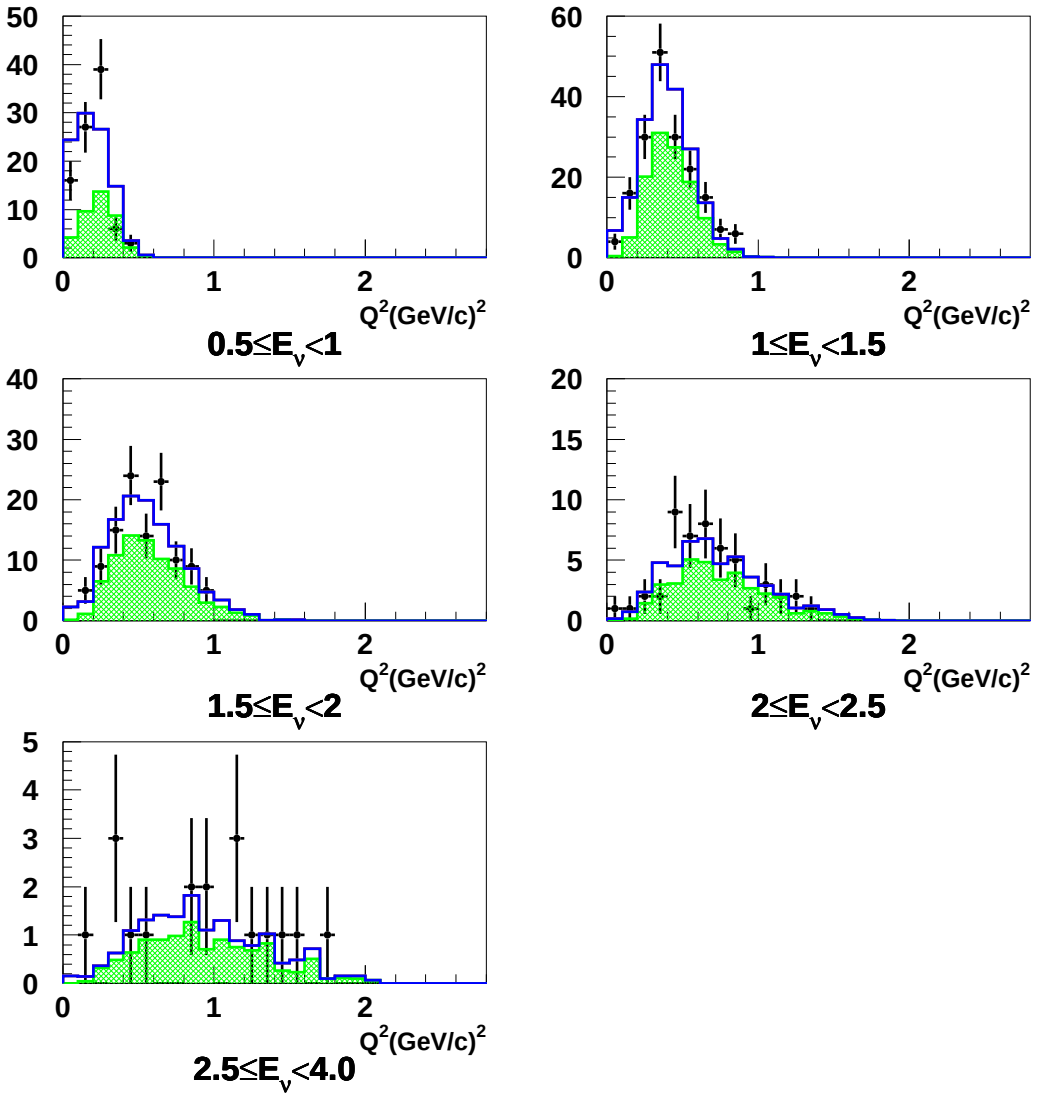

FIG. 9: K2K-IIa 2-track QE q^2 distributions for each observed neutrino energy with the best fit M_A

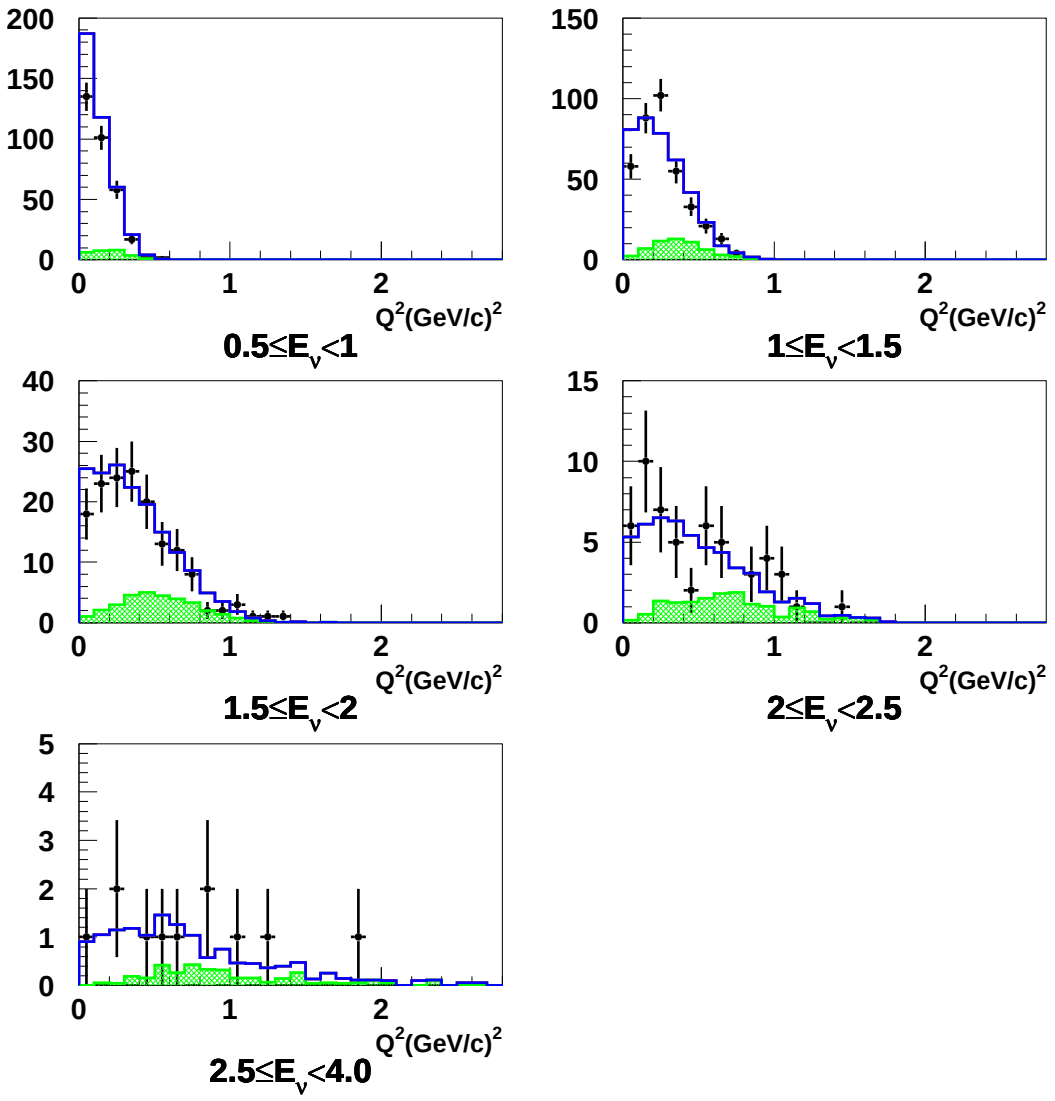

FIG. 10: K2K-IIa 2-track non-QE q^2 distributions for each observed neutrino energy with the best fit M_A

Table of parameters from the fit and also the input parameters.

```
 mrdescale=  0.947
 Chisqr =   126.205251
 Chisqr/NDOF =   1.27480051 99
```

	Value	+Err	-Err	ErrPara	Corr
MA	1.201535	0.157663	-0.148410	0.222933	0.982094
SPECTRUM	1.398622	0.327146	-0.296784	0.332807	0.768563
SPECTRUM	1.159606	0.176777	-0.145615	0.238770	0.976111
SPECTRUM	0.764962	0.147671	-0.124920	0.160088	0.956987
SPECTRUM	1.122544	0.223509	-0.186225	0.282659	0.959071
SPECTRUM	0.842262	0.223793	-0.182326	0.228167	0.870651
PROTON_RES	0.944354	0.082185	-0.082487	0.084080	0.301749
QE/nQE	1.202502	0.210573	-0.183976	0.287225	0.983387

(note, the non-QE/QE is not exactly correct yet, but does not affect the fit)

C. Effect of changing the q^2 cut

In addition to the standard fit, in which we exclude data with q^2 less than 0.2 $(\mathrm{GeV/c})^2$, we examine how the fit changes with different values for this cut, shown in Fig. 11. When only the higher q^2 data is included, the fit results are consistent. If the q^2 distribution did not closely resemble a dipole, or if there was some systematic problem with our analysis, we might see a trend, but no such trend is apparent.

When the fit is extended to include all the data, shown by the data points at low q^2 min, the fit value is systematically higher. However, we understand that there is a significant discrepancy between our Monte Carlo and the data in this region. It is unlikely that this discrepancy is due to the value of M_A, but due to some other aspect of the interaction model or the nuclear effects. We do not consider this to be an uncertainty in the M_A fit value at this time, but an indication of an effect that merits more careful study.

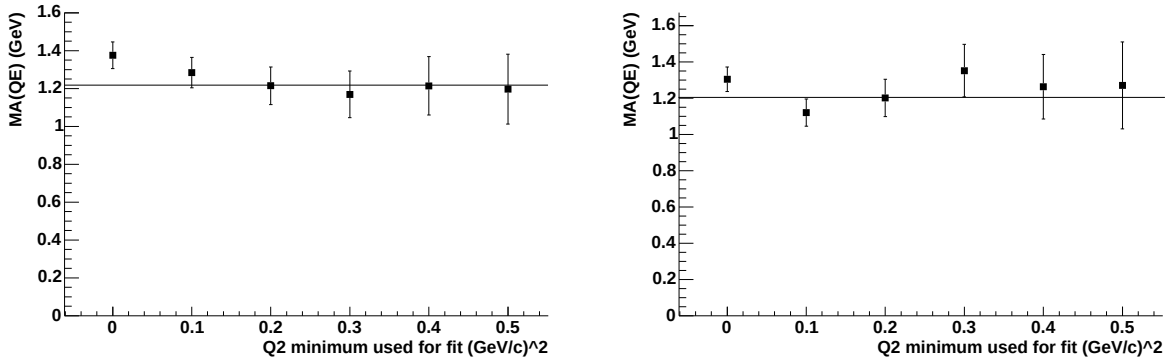

FIG. 11: The variation of the fit value of MA with different values for the minimum q^2 cut. Left is K2K-I data, right is K2K-IIa data. The uncorrelated errors shown include statistical and flux free parameter errors.

D. Fit the shape of each energy region separately

Since we divide our data into five energy regions, we can perform an important consistency check by fitting each energy region separately. The results are shown in Fig. 12. At high energy, variation is within the statistical and systematic errors. The energy bin between 1 and 1.5 GeV is consistently low, for K2K-I it is significantly low. Take together, these plots suggest a systematic effect at lower energy. There is a related systematic effect regarding the data fit with and without the MRD-1L events. The MRD-1L events leave hits only in the first x and the first y layer of the MRD and have a lower momentum than the MRD-3D sample. The MRD-1L sample is described in more detail in the subsection about the event selection uncertainty with the other systematic errors.

E. M_A fit using E_ν shape from merged spectrum analysis

In this analysis, the flux of neutrinos at each energy is a free parameter. This means that the shape of the q^2 distribution is fit at each energy. Another technique would be to take the shape of the energy distribution to be the one reported by the near detector merged fit, and only allow the overall normalization and the nQE/QE fraction to be free parameters. This is still, in some sense, a shape fit because the normalization is free, even if the normalization for individual energy regions is not.

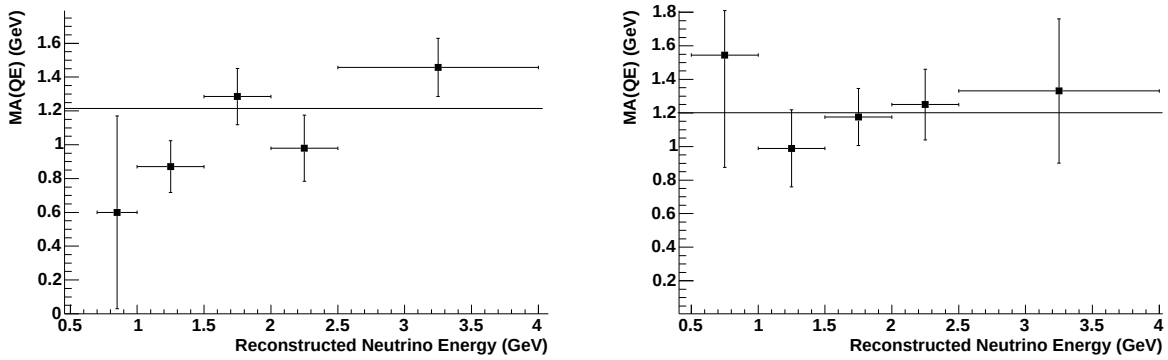

FIG. 12: Values of M_A, fit separately for each energy region. Left is K2K-I data, right is K2K-IIa data. The errors are statistical and energy flux free parameter errors.

Eun Ju Jeon performed this kind of fit more than two years ago. I have updated it to include the Fall 2004 merged fit results. For these results, the parameters for the flux at each energy are allowed to vary, but are constrained to be within the errors from the merged fit using an additional chisquare term. The exception is the flux from 1.0 to 1.5 GeV which is fixed at 1.00. The overall normalization is allowed to vary instead.

The result for K2K-I is 1.18 ± 0.09. For K2K-IIa I get 1.09 ± 0.14. The chisquare value is somewhat worse than the equivalent cases. [Make a table of these results.] The uncertainty includes only the parts incorporated into the Minuit fit: The nQE/QE ratio, the normalization, the constrained flux parameters, proton rescattering, and the statistical error. It is important to emphasize that the values for the flux parameters and the energy scale from the merged fit depend on the choice of M_A in the Monte Carlo, so this result has some additional uncertainty. I am currently repeating the rest of the systematic studies.

VI. SYSTEMATIC EFFECTS

We have performed studies of systematic errors and a large number of simpler consistency checks. They are summarized in the Tab. IV and then described in more detail with supporting data, plots, and examples in the text that follows. The effects highlighted in this table are the most significant, or are of special interest.

Source of uncertainty	K2K-I	K2K-IIa	how it was estimated
STATISTICS	**0.03**	**0.04**	Minuit fit.
MC statistics	0.01	same*	Divide data in half, retest.
Interaction model			
SINGLE-PION MA	**0.03**		Compare Neut samples or Neut re-weighting
FORM FACTORS CCQE	**0.07**	**0.08**	McConnel/Jeon analysis. Its a shift.
nQE/QE	**0.03**	**0.05**	Free parameter in Minuit fit
Coherent pion	< 0.01	< 0.01	Turn off correction, also turn off completely.
Deep inelastic scattering	0.02	0.02	Turn off Bodek Correction
Form factors single-pion	–	–	We use Neut default values.
Nuclear model			
PAULI BLOCKING	**0.01**	same	This is the choice of k_f for Fermi gas model
Proton Rescattering	0.02	0.02	E.J.Jeon analysis, free parameter in fit
Momentum distribution (cross-section)	< 0.02	same	Studied true q^2 distribution
Momentum distribution (kinematics)	< 0.03	same	Studied reconstructed q^2 distribution
Fermi gas model – choice of E_B	0.02	same	Reconstruction and kinematics
Pion Absorption	–	–	Not studied
Experimental effects			
MUON MOMENTUM SCALE	**0.09**	**0.09**	1% change in escale = 6% change in M_A
RELATIVE FLUX	**0.08**	**0.10**	Five parameters in Minuit fit
EVENT SELECTION	**0.06**	**0.01**	Compare MRD3D+1L with MRD3D only
Acceptance and efficiency	0.02	same	Checked method only
Aluminum	–	–	Included in the estimate of Pauli blocking
Other consistency tests			
Energy effect	**0.10**	**0.10**	Fit only low bins or only high energy bins.
Run analysis on MC	0.01	0.01	Yes, default result is reproduced.
Compare K2K-IIa and K2K-I result	–	–	0.01 Consistent. Surprisingly close.
Compare halves of K2K-I data	0.01	–	
delta-theta cut	0.01	same	change 25/30 to 25/25
Binning	<0.01	same	E.J.Jeon Analysis
q^2_{min} cut	–	–	Low q2 causes shift to higher M_A

TABLE IV: Summary of uncertainties in M_A analysis. * "same" assumed equal to K2K-I

A. Statistics

1. Statistics

The statistical error is found by rerunning the Minuit fit for M_A with all the other free parameters fixed to their best fit value. In this case the uncertainty for 2001 data is 0.03 and for 2003 data is 0.04. This is an estimate, if the statistical errors were the dominant error (they are not) we would determine this value more carefully.

In addition to the results reported by Minuit, we have checked that the data contains no large systematic bias with respect to time or data set by performing fits separately on the first half and second half of the K2K-I data and also on the K2K-IIa data. For the former, the results are within 0.01 of the full fit value. For the K2K-IIa data, there is a systematic bias toward lower M_A value when we reanalyze using half the events. This effect is due to small number of events per bin, especially for the high energy bins, or possibly due to smaller MC statistics in each bin (see next section). Rebinning the data using q^2 bins of 0.02 instead of 0.01 $(\mathrm{GeV/c})^2$ yields values consistent with the full data and smaller bin size.

In some ways, the uncertainty I have labeled "relative flux" (described below) also behaves as a statistical error. I mean this in the sense that it causes the error to be scattered above and below the central value, and it decreases with increasing statistics. This was checked using a virtual MC experiment with different sized fake-data samples. But it is a systematic error, if the relative flux could be constrained, the resulting contribution to the total error would be reduced. It is quantified separately, and is described in more detail in its own section below.

2. MC statistics

This was estimated simply by dividing the MC samples in half and running the analysis separately for each half, using the same data. For K2K-I samples with more than 10 MC events per 1 data event, the results are within $\pm$ 0.01. For samples with less MC statistics, there is a bias toward smaller fit value of M_A due to statistical problems calculating the acceptance and migration. It was found that 5 Monte Carlo events for each real event was certainly inadequate for K2K-1 data.

B. Interaction Model

1. *Single-pion M_A*

Just as the M_A^{QE} is uncertain and measured only in neutrino beam experiments, inspiring us to measure it with the SciFi detector, likewise the single-pion M_A ($M_A^{1\pi}$) is best measured with neutrino beam experiments. We do not measure $M_A^{1\pi}$ at this time, rather we estimate the systematic uncertainty it contributes to M_A^{QE}.

We take the default NEUT value of $M_A^{1\pi} = 1.1$ GeV/c^2 and consider this value to be uncertain by 0.1 GeV/c^2. By comparison, previous bubble chamber measurements of this value give $M_A^{1\pi} \sim 1.15 - 1.2$[18], though these results have recently been reexamined [citations?] To test this systematic effect, a complete MC was generated using the alternate value 1.2 GeV/c^2, and the fit result was compared with the regular result.

We quote our uncertainty due to $M_A^{1\pi}$ to be the difference between the two Neut MC samples that we have run completely through our detector simulation: $M_A \pm 0.03$. It should be noted that the fit with the higher M_A still yields a reasonable fit to our data. [Quantify this!] The previous Neut 43 re-weighting studies by E.J. Jeon give a similar estimate for the uncertainty, shown in Fig 13. We hope to add another value $M_A^{1\pi} = 1.00$ with the full detector simulation to further check this result, and to look for asymmetry in this uncertainty.

2. *Form factors CCQE*

New data in the past decade, and in particular new data in the past couple years from electron scattering experiments at JLAB have allowed for improved parameterizations of the CCQE form factors G_E^N, G_M^N, G_E^P, G_M^P, which are used in the calculation of the CCQE cross section. See the citations in [12, 13] for reference to the experimental results. The previous assumption was that these form factors had a dipole shape, except for G_E^N which was taken to be zero. The nuclear physics community is working toward a consensus on the correct, improved description of these form factors, based on these new data. Because this changes the shape of the q^2 distribution, it has an effect on the fit values of M_A.

An initial analysis of the effect of these improvements has been described by Sakuda, Walter, McConnel, and Jeon at previous collaboration meetings and have been repeated

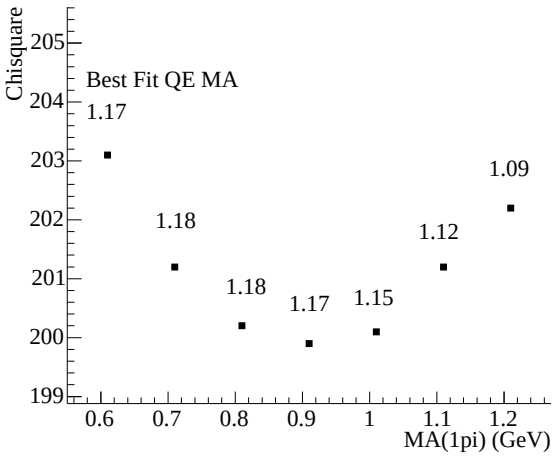

FIG. 13: Jeon's method of re-weighting the Neut43 vectors gives the same ± 0.03 uncertainty, assuming $M_A^{1\pi} = 1.1 \pm 0.1$. [11]

with this updated analysis. The shift observed is 7 or 8%. Because this analysis recalculates the CCQE cross-section from scratch, I have simply replaced the old cross-sections with the calculation by Bosted [12] or alternatively by Budd, Bodek, Arrington [14]. The difference in shape of the q^2 distribution is shown in Fig. 14 for M_A=1.1 and $E_\nu = 1.2$.

One uncertainty remaining is due to the discrepancy between the cross-sections calculated from electron scattering experiments using Rosenbluth extraction and results from polarization transfer data. This is described in all the citations and BBA-2003 gives parameterizations from the cross-section alone, and from the combination of the two. The difference for the M_A fit is negligible, the quoted result is based on the combined fit. In the context of the MA analysis, the older parameterizations of Bosted give a result very similar. For both parameterizations I am using the Galster[15] parameterization for G_E^N.

The conclusion is that the best value for M_A is based on the new vector form factors, while the other value should be retained for comparison with older M_A analyses. However, at this moment we still quote the value obtained using the old form factors.

M_A fit value	K2K-1	K2K-IIa
dipole factors	1.21	1.20
Bosted	1.15	1.13
BBA 2003	1.14	1.12

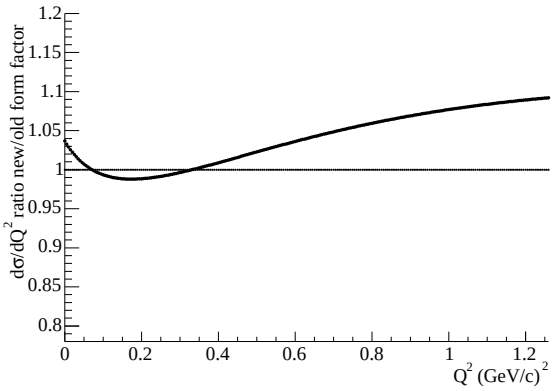

FIG. 14: Ratio of cross-section for (new form factors)/(old dipole form factors). $M_A = 1.1$ GeV/c^2 and $E_\nu = 1.2$ GeV. There is a change in normalization in addition to a change in shape.

3. non-QE/QE ratio

The non-QE/QE ratio is a free parameter in the M_A fit, labeled by the parameter B in equation [ref equation] and listed in the table with the results. By itself it contributes roughly 0.03 uncertainty to the fit value, though the actual effect is correlated with the flux errors, and that correlation is included in the final uncertainty.

4. Coherent pion and DIS

We apply the coherent pion following Marteau's prescription [17] and Bodek/Yang's deep inelastic scattering (DIS) corrections [16], as is done for the K2K energy spectrum and oscillation analysis.

The DIS correction re-weights all DIS events by the following formula involving q^2:

$$weight = q^2/(q^2 + 0.188).$$

It affects the entire q^2 region of interest in this analysis, though the correction is most significant at low q^2. This is an approximation to the complete description to the DIS correction. When the DIS correction is turned off, the fit value changes by 0.02.

The coherent pion re-weighting is given by the following polynomial in neutrino energy,

$$weight = -0.00483E_\nu^4 + 0.08058E_\nu^3 - 0.4838E_\nu^2 + 0.247E_\nu - 0.2149.$$

Again, all coherent pion events are re-weighted by this fraction. The coherent pion events have such a small fraction for $q^2 > 0.2$ that the effect of turning off the correction completely (or turning off all coherent pion events completely) has a negligible effect on the M_A fit.

Only the coherent pion effect is significant for fits that include the low q^2 region. In this case, zero coherent pion in the MC reduces the fit value of M_A by 0.10.

[Please include a plot demonstrating these effects and corrections visually.]

5. Form factors single pion and resonance production

Single pion production, including the production of a delta and other resonances, are expressed in terms of form factors similar to the ones for CCQE. The uncertainties in this model have not been analyzed. We simply take what Neut reports, using the different values of $M_A^{1\pi}$ available.

C. Nuclear Model

One general comment. This is an active area of study, with many recent papers and even a series of workshops devoted to it. There is significant theoretical uncertainty about the magnitude of the effects described here. However, the existence of these effects is certain. We do not consider all possible models for these effects, and we are not attempting to present a measurement of any of them. Using some reasonable assumptions, we have quantified how the nucleus modifies the shape of the q^2 distribution and the effect it has on the measurement of M_A.

Three types of nuclear models have been seriously considered. The current official model treats the nucleus as a uniform Fermi-gas. Because of its simplicity, almost all neutrino interaction Monte Carlo in current experiments use this, despite some known limitations. This replaced a model where the nucleon momentum distribution was based on Brevia [21]. Work is under way by many people to create a Monte Carlo that uses the spectral function model of Benhar [22], which has yet a different nucleon momentum distribution and also naturally includes nucleon-nucleon correlations. These three distributions, shown in Fig. 15, are very different. Most of what is described here is based on the official Fermi-gas model, but for the M_A analysis, the others are considered and the effect on the results is surprisingly small.

1. Pauli blocking: Fermi gas model – choice of k_f

This was studied originally by Jeon and was revisited again by Gran using the calculations of H. Nakamura. The value of the Fermi-momentum k_f is the upper limit on the nucleon momentum in the Fermi gas model, and affects the shape of the momentum distribution as well as its average value. However, for quasi-elastic interactions, the only significant effect it has is the amount of Pauli blocking; it has no effect for fits with $q^2 > 0.2$. This was confirmed by substituting alternative values for the amount of Pauli blocking into the CCQE cross-section calculation, and the fit result changed negligibly.

Within the context of the Fermi gas model, Table V shows some values for k_f (and also for the binding energy, discussed later). We take k_f to be 225 for oxygen.

There is also an effect on the single-pion (resonant pion) background. The overall amount

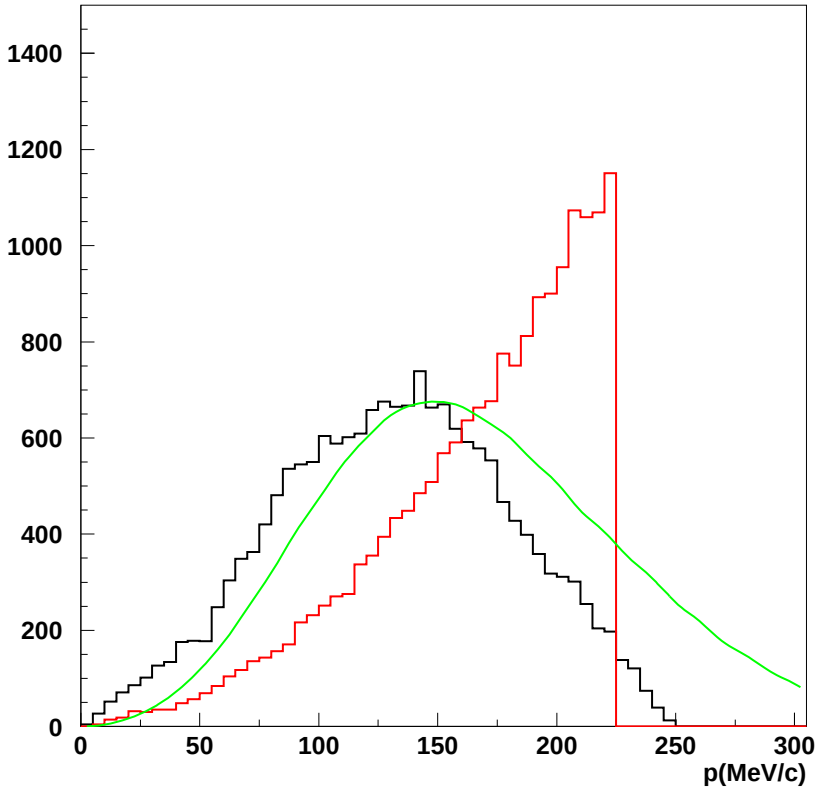

FIG. 15: Fermi-momentum distributions for Neut 4.3 (black) based on Brevia, et al., Fermi Gas Model (red) as implemented in Neut 4.5, and the spectral function calculation (green). There are differences in the average momentum and also in the shape of these distributions.

nucleus	^{6}Li	^{12}C	^{24}Mg	^{40}Ca	^{59}Ni	^{89}Y	^{119}Sn
k_F(MeV/c)	169	221	235	249	260	254	260
ϵ_B (MeV/c)	17	25	32	33	36	39	42

TABLE V: Fermi momentum k_F and effective average potential ϵ_B for various nuclei. these values were obtained from an analysis of quasi-elastic electron scattering at beam energies between 320 MeV and 500 MeV and at a fixed scattering angle of 60 degrees [1, 6]. The errors are approximately 5 MeV/c (k_F) and 3 MeV (ϵ_B).

of Pauli blocking for single pion interactions is less than for quasi-elastic interactions, but the suppression factor (the percentage of interactions blocked) is actually higher for interactions

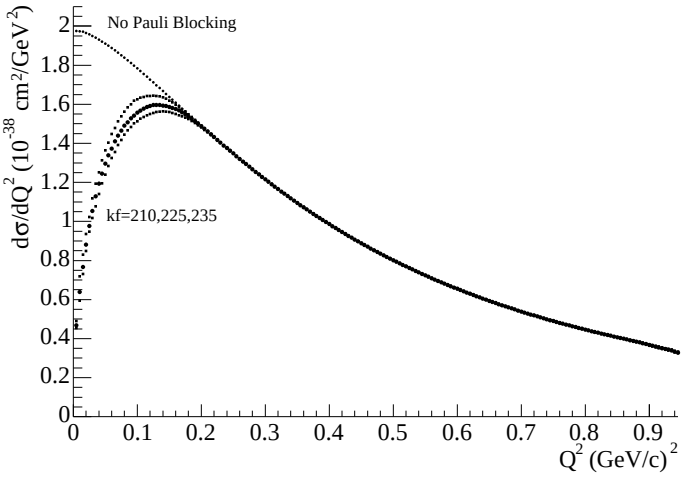

FIG. 16: Comparison of Fermi gas model with no Pauli Blocking and the same model with Pauli Blocking and three choices for the value of the Fermi Momentum k_f.

with $q^2 > 0.2$. The amount of blocking just above this value of q^2 is a couple percent. Because even this is so small, the total effect due to uncertainty in Pauli blocking can be no larger than 0.01, which has been tested by applying a correction to the background. Pauli blocking for these is somewhat more difficult to calculate because the many different resonances must be treated individually, but despite the resulting uncertainty, the effect is small.

For fits over the entire q^2 range, this becomes a dominant uncertainty. Adjusting the total amount of Pauli-blocking (the percentage blocked) by 10% causes approximately a 0.10 change in the MA fit value. The effect is much smaller when a q^2 cut of 0.10 is used.

Also, a different nuclear model, such as the spectral function model with its higher momentum distribution, may give significantly different amounts of Pauli blocking. In the spectral function model, Pauli blocking is particularly difficult to calculate. Most calculations follow the Fermi gas approach and the result would be the same as above, but the spectral function should have a larger percentage of high q^2 events blocked, simply because there are more nucleons with higher momentum. In this case, the simplistic calculations still give no effect for the $q^2 > 0.2$ fits used in this analysis.

2. Fermi gas model – choice of E_B

The uncertainty in the nuclear binding energy within the Fermi gas model has several kinds of effects. The analysis of these effects is not yet complete, but I will summarize the progress here. In our simulations and reconstruction we take the nuclear binding energy to be 27 MeV, following the data in Tab. V. [Note, SciFi uses 30 MeV for much of its reconstruction.]

In this case, the uncertainty in this value affects our reconstruction through the formula to calculate the neutrino energy and the q^2 for the interaction. An uncertainty of 3 MeV would look like an energy scale error of 0.3%, which would cause a 2% error on the fit value of M_A.

The binding energy is also part of the Neut simulation, in addition to part of the reconstruction. It modifies the kinematics of the outgoing particles.

Finally, it is supposed that the binding energy modifies the cross-section itself in a small way, providing an overall suppression and a slight change in the shape of the q^2 distribution. A description of the possible size of this effect has been calculated by Tsushima, et al., [arXiv:nucl-th/0307013] and later considered by Bodek, Budd, Arrington [arXiv:hep-ex/0309024]. Though my estimate is not yet complete, I expect this to also have a smaller contribution to the M_A fit value.

3. Proton rescattering

[This section will be updated. Please skip it for now.] Proton rescattering inside the nucleus causes changes to the proton angle and the proton momentum. The former will cause a migration between the 2-track QE to the 2-track non-QE samples, while the latter will cause a migration from both to the 1-track sample. In the Neut Monte Carlo, the amount of rescattering is based on the results of proton scattering experiments[citation]. The Monte Carlo was re-weighted to account for variations in this parameter, and was studied by Jeon and reported in her thesis. We use 0.87 ± 0.07 of the amount used in NEUT. [This number needs to be checked carefully. This was based on a very early version of the spectrum fit result? Or some beam test?] The amount of proton rescattering is a free parameter, and the deviation from this central value with this error is added to the total chisquare. The fit

results are included in the result tables.

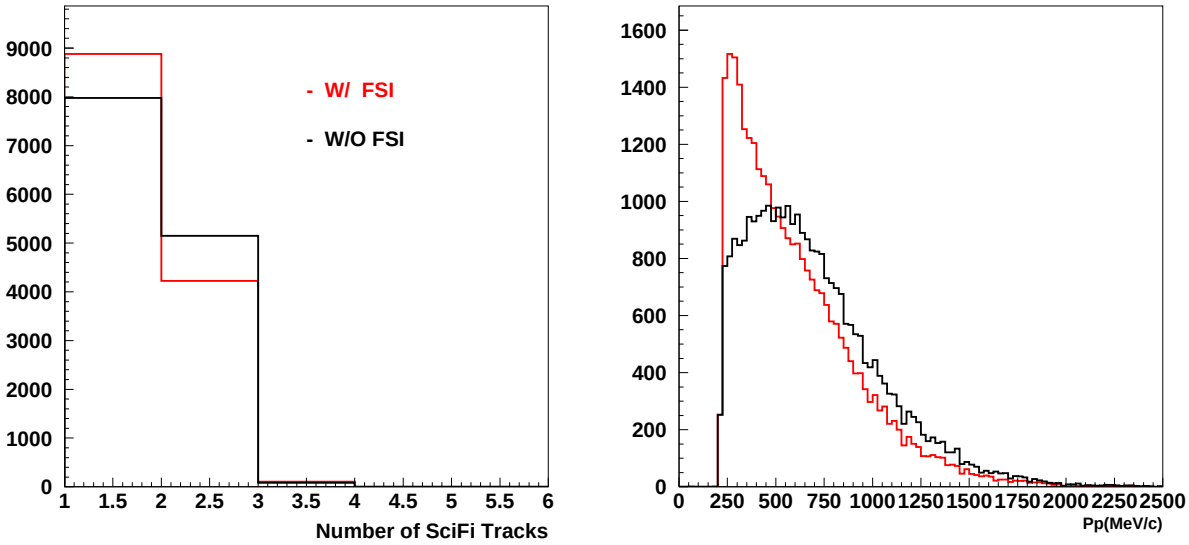

FIG. 17: Update these figures if possible. The left figure shows the difference between the default amount of proton rescattering and zero rescattering on the number of tracks observed in SciFi. The right figure shows how the proton momentum is transformed, which affects whether the second track is observed. There are also effects on the angle of the proton.

4. Nucleon momentum distribution - general considerations

I have some general comments about the effect of the nucleon momentum distribution. There are in general two kinds of effects: the shape of the true q^2 distribution (and also an overall suppression), and an effect on the reconstructed q^2 distribution. This second effect is because our formula to calculate q^2 is based on a calculation of E_ν which differs from the true E_ν because we can not take into account the (unknown) nucleon momentum on an event by event basis.

I refer to these two kinds of effects as "cross section" effects and "kinematic" effects, and have made estimates of how the M_A fit value changes. The first is studied by considering changes in the shape of the true q^2 distribution. The second causes a different reconstructed q^2 distribution, and is an independent effect. Also, the uncertainty in these effects might apply separately to the CCQE signal as well as the single pion background.

5. Nucleon momentum distribution - CCQE cross section

For CCQE events, the effect of this was analyzed in the following way: H. Nakamura provided us with calculations of the cross section using the Fermi gas model under several different conditions. With the calculations using different k_f it was observed that there was no difference for the $q^2 > 0.2$ fits. He also included a calculation using the spectral function momentum distribution of Omar Benhar[22], which is an alternative to the Fermi gas model. These calculations show that there is a small adjustment in the CCQE cross-section and a small difference in the shape over the entire q^2 range, which is estimated to have an effect of 1% on the M_A fit value. The only significant difference is the amount of Pauli blocking at low q^2, which is already known to not affect the fit value in this analysis.

I also considered another alternative model, the one used in Neut version 4.3. The change in the shape of the q^2 distribution leads to an uncertainty of 1% on M_A. Like the calculations of Nakamura, this is based only on the true q^2 distribution, and does not include kinematic or detector effects.

The method to obtain these values is as follows. Consider any effect that produces a change in the shape of the q^2 distribution for $0.2 < q^2 < 1.2$, either for QE signal or for non-QE background. See the left plot in Fig. 4 or Fig. 14 for examples. This can be approximated as a simple change in linear slope over this region. That change is, to first order, directly related to the change in fit value for M_A. In this way, any model that can be expressed in this form can be quickly tested to estimate an uncertainty in the final fit value.

There are interesting effects, certainly for CCQE, at high q^2, where the tail of the nucleon momentum distribution causes significant discrepancies in the cross-section. For our analysis, our data does not have enough statistics to make any statements or contribute to an uncertainty. However, these effects are likely to be of interest to higher statistics experiments, or experiments whose neutrino energy (and therefore the q^2 distribution) is higher, and will need to be considered more fully in the very near future.

6. Nucleon momentum distribution - single pion cross section

As in the previous section, there is an effect for single pion events which are the background to the analysis. If the shape of the background changes, the resulting fit value of

the CCQE M_A will change.

In this case, only two momentum distributions are available, the current official value from Neut version 4.5, which is a Fermi-gas model, and the previous version of the Neut Monte Carlo (version 4.3) which implemented a distribution by Brevia [21]. Except for different amounts of Pauli blocking at low q^2, there is no effect on the true q^2 distributions.

7. Nucleon momentum distribution – single pion kinematics

Unlike the CCQE form factors, which affected the true q^2 distribution, I now want to consider an effect primarily in the reconstructed q^2 distribution. Even if the cross section for $M_A^{1\pi}$ remains the same, the kinematics of the outgoing lepton are different because the nucleon momentum distribution has changed.

This is studied suing a special set of Neut interaction vectors prepared with an identical single-pion cross-section, but the alternative nucleon momentum distribution based on Brevia. In this case, the true q^2 distributions are the same, but the distribution of the reconstructed q^2 distributions are different. I observed a change in shape of 4% (i.e. the slope of the right hand plot in Fig. 18) which thus corresponds to a change in the fit value of M_A of 2%. The smallness of this result is significant. The Brevia distribution and the Fermi Gas distribution shown in Fig. 15 are very different. The average momentum is significantly lower for Brevia, and the shape is very different. Despite these enormous differences, and regardless of which distribution is the most accurate description of the nucleus, the effect on the MA analysis is surprisingly small.

8. Nucleon momentum distribution – CCQE kinematics

At this point, separating out kinematic effects in the CCQE q^2 distribution has been more challenging, and is not completed. However, in the context of this analysis, these other contributions are small compared to the other uncertainties, and I expect that this remaining contribution is also small.

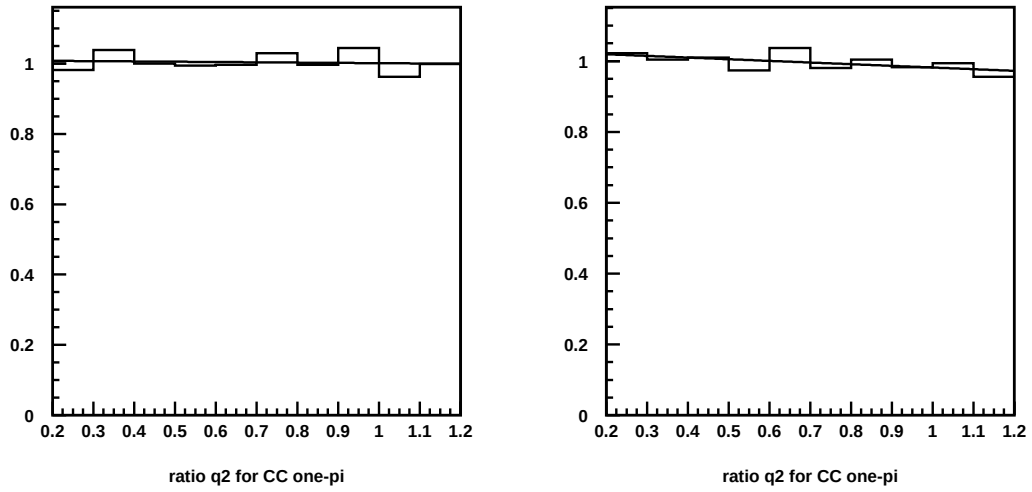

FIG. 18: The left shows the ratio of the true q^2 distribution, Neut old/Neut official. The right shows the same ratio for the reconstructed q^2 distribution.

9. Pion absorption

This is included in the Neut Monte Carlo. Its uncertainty and effect on the M_A fit is not studied. In principle it also causes a migration of events to and from the one track and two track samples, similar to the effect of proton rescattering.

D. Experimental Effects

1. *Muon momentum scale*

The shape of the q^2 distribution is very sensitive to the uncertainty in the muon momentum scale. In the fine grained detector systems, the muon momentum is calculated using the range measured from the reconstructed interaction vertex to endpoint in the MRD. This is accomplished using a look-up table based on the Monte Carlo simulation, which in turn is based on the dE/dx through all the material of the detectors. On an event by event basis, this measurement has an uncertainty of $\pm$ 80 MeV or so, based on the segmentation of the MRD. What is of concern here is a possible shift (MC relative to data) of the average value, a shift in the overall scale of this momentum measurement. If this scale is off by 1%, it causes a shift of 6% shift in the value of M_A, shown in Fig. 19 for K2K-IIa data. Also, this correlation is strong enough that the M_A fit, with its other free parameters, does not provide its own constraint on this parameter. Thus, the absolute calibration of the detectors is particularly important.

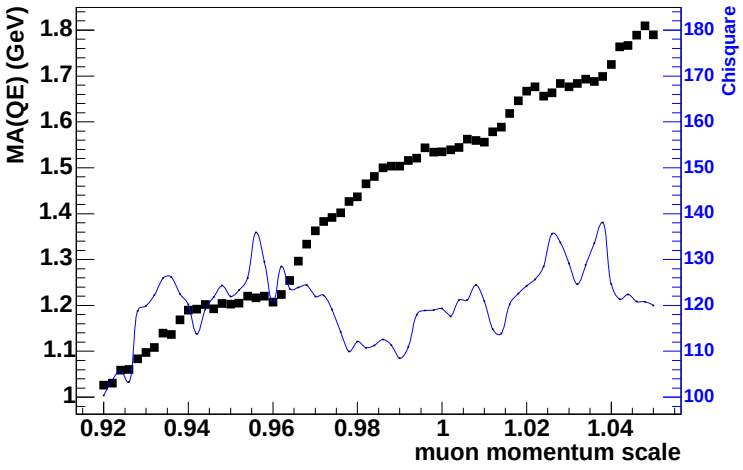

FIG. 19: Effect of scaling the MRD muon momentum. M_A fit value and the fit χ^2 are shown. This is for K2K-IIa data. The fit begins to break down, probably because of binning, at low values of momentum scale.

In principle, errors on the momentum scale could come from the way any of the detector sub-systems are modeled. For the K2K-IIa data set, things are simpler because there are

only three significant components: the MRD detector, the SciFi detector, and the mini-SciBar detector. For most tracks, the MRD detector accounts for the majority of dE/dx, so it is the most important. For the K2K-I data, the Lead Glass detector also plays a significant role.

In the SciFi spectrum fit analysis, these two pieces, MRD and Lead Glass, are treated separately. The results from the spectrum fit are used in the M_A analysis, but with some care. In the spectrum fit, these two momentum scales are free parameters in a fit of the muon angle and muon momentum distributions. This technique is very similar to the M_A analysis and it uses the same data set. It is certain that other uncertainties, such as M_A itself, are affecting the momentum scale values obtained. Simply using these scale results in the M_A fit will bias the M_A result. This bias has been estimated by rerunning the spectrum fit after re-weighting the MC with different M_A^{QE}. The value of the momentum scale varied by $\pm$ 0.02 for re-weighting factors for M_A^{QE} between 0.90 to 1.40, when applied to the K2K-IIa fits. Based on this, an additional systematic error of 0.01 is assigned. It was also observed that the chisquare for the spectrum fit improved toward $M_A^{QE} = 1.30$, though values between 1.1 and 1.4 were all acceptable, between 88 and 90 for (86-13 dof).

Using the neutrino data to calibrate the momentum scale is the most accurate measurement we have, from a statistical point of view, though it may have larger systematic errors coming from correlations with uncertainties in neutrino interaction cross-sections. A summary of the reported measurements of the different momentum scale values is given in the Tab. VI. There is some disagreement among the results from each detector group, though in principle each value accounts for a different subset of detectors whose momentum scale can differ significantly.

2. Flux uncertainty

For the shape fit, we allow the flux to be a free parameter for five different energy regions as follows (GeV): (0.5-1.0), (1.0-1.5), (1.5-2.0), (2.0-2.5), and (2.5-4.0). In this way we have minimized or eliminated the potential errors due to the uncertainty in the relative flux from the beam Monte Carlo.

Ignoring the correlation with other systematic errors, I estimate from the Minuit error results that we have a systematic uncertainty of 0.08 for K2K-I data and 0.10 for K2K-IIa

Source	value error	method
SciFi K2K-I MRD	0.950 ± 0.005	spectrum fit
SciFi K2K-IIa MRD	0.947 ± 0.011	spectrum fit
SciFi K2K-I LG	0.950 ± 0.014	spectrum fit
SciFi LG	0.950 ± 0.05	beam test
SciBar Total	0.980 ± 0.003	spectrum fit
MRD	1.000 ± 0.027	material assay
MRD	1.035 ± 0.06	beam test
MRD	0.990	fit neutrino data

TABLE VI: Value for different muon momentum scales. Each is expressed as MC/data. The uncertainties from the SciFi fits are propagated to the uncertainty in M_A value.

data. This is our largest source of uncertainty.. The final calculation of the systematic uncertainty includes the Minuit reported correlation with the other systematic terms.

An important note, this error behaves in many ways like a statistical error. Higher statistics cause this error to be somewhat smaller. This can be supposed by the different values for the K2K-I and K2K-IIa data sets, and is also apparent when testing the M_A fit results for different q^2 minimum cut values. This was further studied by running a virtual MC experiment on different sized samples of fake data and observing the results of many such fits. They were scattered around the central value, as expected, and if the size of the sample is increased, the scatter is reduced.

However, the uncertainty also decreases if the relative flux normalization can be constrained. Thus, the analysis can be significantly improved if accurate, independent knowledge of the neutrino flux is available, such as is expected from HARP.

3. Event selection

The SciFi analysis of K2K-I data use events that penetrate the MRD detector far enough to produce a 3D reconstructed track and also events that only produced hits in the first layer (1L events). This event sample is checked to ensure that there is little contamination from pions passing through the lead glass. Similarly, the analysis of K2K-IIa data uses only

MRD-3D events. A reasonable alternate choice for K2K-I might be to give up the additional statistics and choose only the MRD-3D events. Choosing this alternative causes a shift of 0.06 (MRD-3D only is higher). Similarly, for K2K-IIa, including the MRD-1L events causes a shift downward by 0.01, but it is noted that the lower muon momentum threshold for K2K-IIa (because there is no Lead Glass or SciBar) causes much of the 1L sample to have a reconstructed neutrino energy below 500 MeV, which is below the lowest energy used in this analysis. The mechanism that causes the shift in K2K-I might actually be the same in K2K-IIa but this 500 MeV threshold masks it.

In addition to quoting these numbers from the consistency check, this same effect may be related to the low second data point, the 1.0 to 1.5 GeV bin, in the plot of M_A for each energy,Fig. 12. One note, I naively expected this to be affected by or correlated with the muon momentum scale parameters, but a quick check found this to not be the case.

There is indication is that there is some difference between the low and high energy events, when the data and Monte Carlo are compared. Our Monte Carlo predicts that the low energy (< 1.5 GeV) neutrino events in the 1L sample has a "harder" q^2 spectrum (more high q^2 events, and relatively more low-momentum muons) than the MRD3D sample, see Fig. 20. Further, the higher energy (> 1.5 GeV) 1L events always add to the data at moderately high q^2 such that the overall q^2 distribution is also "harder". If the discrepancy is simply because there are too many 1L events in the MC, this will trivially cause a shift in the fit value of M_A downward when the 1L events are added to both samples.

The actual situation is more complicated, because the relative amounts of 1L events and 3D events at each energy are similar, but the relative amounts of both are different at low energy and at high energy. This latter effect is, in principle, accounted for with the free parameters for the relative flux in both the M_A analysis and the spectrum fit, and should not present a problem here, indicating that the observed low energy discrepancy is related to some other aspect of the neutrino interaction description, or possibly the detector simulations.

One possibility is that the 1L events sometimes have a third hit in the second layer of the MRD, but the path length (and therefore muon momentum) is calculated assuming only the two hits in the first layer. Recently, the SciBar group has changed their p_μ estimate to include the information about this second-layer hit. I have not been able to check this to see if it accounts for the discrepancy.

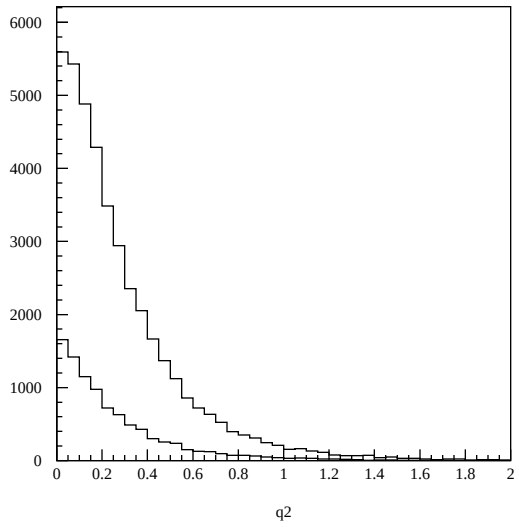

FIG. 20: Difference in the shape of q^2 for MRD3D and MRD1L samples, from MC. Upper line is MRD3D, lower line is MRD1L. The MRD1L line is less steep – it has relatively more high q^2 events. The uncertainty in the relative fraction of these two quantities in the MC will cause an error in the shape of the predicted q^2 distribution.

These preceding two observations indicate that something is described incorrectly, but whether it is in the detector simulation or the neutrino interaction is not apparent. At this time we use the official data samples and include this discrepancy in the uncertainty.

One final thing to note, there is also a sample of MRD events, about 15% of the total, that have a long track reconstructed in either the X or the Y projection, but no track in the other projection. Usually, the other projection does have one or more hits in that projection, but not enough to satisfy the tracking criteria. Work is underway to study and possibly recover this sample.

4. Acceptance or efficiency

We have used two different methods to calculate the acceptance and also the migration of true-values of E_ν and q^2 to their reconstructed values based on the Monte Carlo. Because the analysis performs its own calculation of the CCQE cross section in order to allow M_A to be a free parameter, these true values for the q^2 and E distributions must then be converted

to what the physical SciFi detector will see.

The first is the original method used by Eun Ju which considers acceptance and q^2 migration in a simple way. The second, improved version considers the q^2 migration and includes migration among the energy bins.. This second version more accurately represents the results of the Monte Carlo, but is much more sensitive to the Monte Carlo statistics.

In general, with the MC statistics we use, these two methods produce M_A fit results that disagree by 0.01 to 0.03 while they have reasonably similar chi square values. This range depends on the data set being analyzed and was considered for almost every consistency check we have done since Fall of 2003.

Thus we are confident that whatever remaining uncertainty, either in method or statistics, it is less than 0.03. I quote this number here as a consistency check, and do not use this value for calculating the final uncertainty.

In contrast to this procedure, we take the inelastic background to be exactly what is reported by Neut and the detector simulation, so there is no separate consideration of the acceptance for the background, beyond what the full Geant simulation gives.

5. Aluminum

We ignore, at present, the possibility that the aluminum in the detector will be susceptible to different nuclear effects. In particular, ^{26}Al, in the Fermi gas model, will have a higher k_f and ϵ_B, and thus will have more Pauli blocking. However, this effect is within the range of k_f already studied in this analysis. For CCQE events with fits $q^2 > 0.2$ this will be negligible, but for the single-pion background, more Pauli blocking will have some small effect. This total uncertainty is discussed in the Pauli blocking section.

It is known that the nucleon momentum distribution has effects other than those described by Pauli blocking, which may be more significant for $q^2 > 0.2$. There is an overall suppression of the cross section and different distributions also have different high q^2 tails. Differences between Aluminum and Oxygen in this regard have not been closely studied, and the analysis assumes all the targets are in Oxygen nuclei. There will be no water in the SciFi detector for the K2K-IIc run, so we will get some estimate of the effect of aluminum from that data.

6. Fiducial volume and $N_{targets}$

For the shape fit, these are not applicable. The uncertainty here is taken up by the overall normalization factor, which has no effect on the resulting value for M_A.

7. Track finding efficiency

Just as proton rescattering causes a migration from the one-track to two-track samples, also the detector's track finding efficiency, especially the threshold for reconstructing short tracks, may have a similar effect. This effect is not studied.

E. Other consistency checks

General comment. The checks described below were simple tests. Some imply a systematic error, some may be correlated with effects described above, while others suggest simple statistical fluctuations. Some of these tests are one-time only tests and actually represent shifts rather than symmetric errors.

1. Energy effect

Analyzed the shape of the q^2 distribution for each energy region separately. Described in the results section in Fig. 12, and also discussed in the event selection section in relation to the discrepancy when MRD-1L events are considered.

In addition, I also divided the data into two energy regions (instead of five) and fit each separately. This has the advantage that the fluctuations due to a small number of bins has a smaller effect. The low region was from 0.5 to 1.5 GeV (three of the energy regions combined), the high energy region was 1.5 to 4.0 GeV. The results for K2K-I were 1.10 ± 0.07 and 1.18 ± 0.13 and for K2K-IIa 1.13 ± 0.19 and 1.24 ± 0.19. The errors here include only the MINUIT fit errors, for which the statistics and the flux free parameter are by far the largest and are not significantly correlated between the energy regions. This simplifies the same trend observed in Fig. 12.

2. Does the analysis reproduce the MC?

Yes. Several subsets of the MC was extracted and used as a "fake data sample" for a virtual MC experiment. The results, when averaged, reproduce the intrinsic M_A of 1.1 within 1% and the observed fluctuations are consistent with the errors in the fit reported by MINUIT for the real data.

3. Compare halves of K2K-I data

Simply divided the K2K-1 data set in half. The fit values agree within 0.01 This is consistent with our 0.03 statistical uncertainty. The K2K-IIa data set is too small, there is

a systematic bias in that analysis because the statistics of each bin are too low. When the K2K-IIa data is rebinned using coarser bins, the two halves are also in agreement.

4. Delta-theta cut

The delta-theta cut divides the two-track sample into the QE enhanced and the non-QE enhanced data. Delta-theta is the difference between the measured proton angle and the calculated angle assuming the proton is recoiling from a quasi-elastic interaction. Good agreement (small delta-theta) suggests that the interaction was indeed QE, while inelastic events will have a full range of possible angles. Originally the cut was set to maximize the QE and non-QE enhancement, possibly improving the accuracy of the QE/nQE free parameter in the fit. On the other hand, this technique throws out all the events with delta-theta between 25 and 30 degrees.

5. Binning

Our primary analysis uses q^2 bins of 0.1 $(\mathrm{GeV/c})^2$. Eun Ju considered alternate binning of 0.05, 0.2, and 0.5. The results of the M_A fit value varied by less than 0.01. The numbers were [buried in Eun Ju's notebook and in an e-mail I have somewhere, and there is also a plot in Eun Ju's thesis. Redo this as a nice plot.]

I note here that due to limited statistics for our data sample, as is standard practice, the high q^2 bins are grouped into several larger bins. Small changes in how this grouping is selected have a negligible effect. However, it is observed that using half the K2K-2a data sample has a very large effect and requires the data to be rebinned. Even though this is not a problem for our data sets, it must be carefully considered for each new data set, especially if the statistics are poor.

6. q^2min cut

This is already described in results section with Fig. 11. We perform our primary analysis using a q^2 cut of 0.2, and fit only the region of q^2 above that. There has always been a discrepancy between data and Monte Carlo, for all near detectors, for data in the

far-forward region, which is also where the very low q^2 events are.

Theoretically, this is where the effects of the nuclear model and interactions are the most significant. Pauli blocking, coherent pion, and the Bodek DIS correction all effect the region $q^2 < 0.2$. These uncertainties are definitely a factor, even with the possibility that the detector description is correct for forward events.

Nevertheless, we do perform our fits to include some and all of this region. The resulting fit value of M_A is always higher, and the quality of the fit is not as good.

This is also consistent with observations by previous neutrino experiments [18] This does not represent an uncertainty to be quoted in this analysis. Rather, it is guidance that the underlying dipole model or our understanding of low q^2 nuclear effects (or both) are inadequate. We hope the continuing study and presentation of these results will lead to progress in these areas, but a statement of uncertainty here is beyond the scope of the present analysis.

VII. CONCLUSION

We have studied the neutrino-oxygen quasi-elastic scattering, $\nu_\mu + n \rightarrow \mu^- + p$, in the few GeV region using neutrino interactions observed in the Scintillating Fiber detector of K2K neutrino oscillation experiment. We performed a maximum likelihood fit to the data to determine the best fit value for the axial vector mass M_A.

We obtain

$$M_A = 1.21 \pm 0.15 \text{ syst.} \pm 0.03 \text{ stat.} \quad \text{for K2K-I data,}$$

$$M_A = 1.20 \pm 0.18 \text{ syst.} \pm 0.04 \text{ stat.} \quad \text{for K2K-IIa data,}$$

and

$$M_A = 1.21 \pm 0.13 \text{ syst.} \pm 0.03 \text{ stat.} \quad \text{combined data.}$$

The combined result is estimated very simply. The errors which are independent to each data set are statistics, flux free parameter, and the event selection uncertainty; but two of these have a statistical nature. The other errors are common, and are not reduced for a combined analysis. A quick estimate obtained by reducing the statistical-like errors and then taking everything in quadrature gives the estimate of $\pm$ 0.13 above. A more careful estimate is underway.

These data are consistent with previous measurements using other nuclear targets, shown in Fig. 21. The values quoted in this figure assume the old dipole form factors. We also report the result using the new dipole form factors, and find $M_A = 1.14$, 1.12, and 1.13 (and with the same errors as above) for K2K-I, K2K-IIa, and the combined result, respectively.

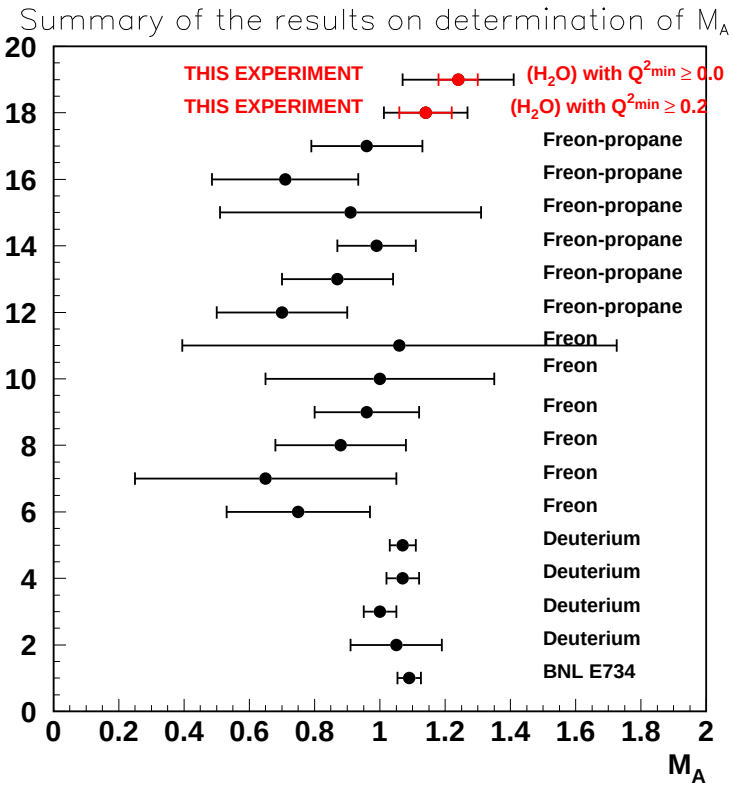

FIG. 21: THIS PLOT MUST STILL BE UPDATED!. A comparison of value of M_A determined in this experiment(red) and values obtained by previous neutrino experiments. For this experiment, red shows statistical errors only, black shows total error.

We have also presented a quantitative study of many significant nuclear effects which are important for measurements like this on heavy nuclei, including our oxygen target. These include the Pauli exclusion effect, other effects of the nucleon momentum distribution, the assumption of a Fermi gas model, as well as the effect of nuclear rescattering of recoil protons.

Acknowledgments

This work was supported by KEK and the KEK-PS group, the Japan Ministry of Education, Culture, Sports, Science and Technology, the Korea Research Foundation, the Korea Science and Engineering Foundation, The U. S. Department of energy, the Japan Society for the Promotion of Science. (Eun Ju should check to make sure I have it all right.)

---

[1] E.J.Moniz et al., Phys.Rev.Lett.**26**(1971)445.

[2] R.A.Smith and E.J.Moniz, Nucl.Phys.**B43**(1972)605.

[3] C.Llewelyn-Smith, Phys. Rept. 3C (1972) 261.

[4] D.Rein and L.M.Sehgal, Ann. of Phys. 133 (1981) 79. D.Rein, Z. Phys. C 35 (1987) 43.

[5] O.Benhar, A.Fabrocini, S.Fantoni, G.A.Miller, V.R.Pandharipande and I.Sick, Phys. Rev. C 44, 2328(1991)

[6] R.R.Whitney *et al.*, Phys. Rev. **C9** (1974) 2230.

[7] S.Hiramatsu *et al.*, Proc. Int. Conf. on Nuclear Structure Studies Using Electron Scattering and Photoreaction, Sendai(1972), 429.

[8] F.A.Brieva and A.Dellafiore, Nucl. Phys. A292(1977), 79.

[9] C.Walter, Nucl. Phys. B (Proc. Suppl.) 112(2002) 140-145. [NuInt01 Tsukuba]

[10] M.H.Ahn, *et al.*, Phys. Rev. Lett. 90, 041801, 2003.

[11] E.J.Jeon, Ph.D. Thesis, 2003.

[12] P.E.Bosted, Phys. Rev. C 51 (1995) 409-411.

[13] E.J.Brash, *et al.*, Phys. Rev. C 65 (2002) 051001.

[14] H. Budd, A. Bodek, J. Arrington, Proc. NuInt02 (Irvine), 2002. [hep-ex/0308005].

[15] Galster, *et al.*, Nucl. Phys. B 32 (1971) 221.

[16] A.Bodek and U.K.Yang, Nucl. Phys. B (Proc. Suppl.) 112 (2002) 70-76 [NuInt01 Tsukuba, hep-ex/0203009].

[17] J.Marteau, have not figured the citation.

[18] T.Kitagaki, *et al.*, Phys. Rev. D 42 (1990) 1331-1338.
T.Kitagaki, *et al.*, Phys. Rev. D 28 (1983) 436-442.
K.L.Miller, *et al.*, Phys. Rev. D 26 (1982) 537-542.

N.J.Baker, *et al.*, Phys. Rev. D 23 (1981) 2499-2505.

[19] B.J.Kim, *et al.*, Nucl. Instrum. Meth. A 497 (2003) 450.

[20] K.Hagiwara, *et al.*, Phys. Rev. D. 66 (2002) 010001 [http://pdg.lbl.gov].

[21] B.Brevia and A.Dellafiore, Nucl. Phys. A 292 (1977) 445.

[22] O.Benhar, *et al.*, Nucl. Phys. A 579 (1994) 493. H.Nakamura and R. Seki, to appear in Proc. NuInt02 converence (Irvine).